Journal of Experimental Botany, Vol. 75, No. 21 pp. 6778–6795, 2024
https://doi.org/10.1093/jxb/erae418 Advance Access Publication 8 October 2024

RESEARCH PAPER

High water use efficiency due to maintenance of photosynthetic capacity in sorghum under water stress

Yazen Al-Salman[1,2,†,*], **Francisco Javier Cano**[1,3], **Emma Mace**[1,4,5], **David Jordan**[1,4,5], **Michael Groszmann**[1,6,7], **and Oula Ghannoum**[1,2]

[1] ARC Centre of Excellence for Translational Photosynthesis, Canberra, ACT, Australia
[2] Hawkesbury Institute for the Environment, Western Sydney University, Richmond, NSW, Australia
[3] Instituto de Ciencias Forestales (ICIFOR-INIA), CSIC, Carretera de la Coruña km 7.5, 28040, Madrid, Spain
[4] Queensland Alliance for Agriculture and Food Innovation, Hermitage Research Facility, University of Queensland, Warwick, QLD, Australia
[5] Department of Agriculture and Fisheries, Agri-Science Queensland, Warwick, QLD, Australia
[6] Division of Plant Sciences, Research School of Biology, The Australian National University, Acton, ACT 2601, Australia
[7] Grains Research and Development Corporation (GRDC), Barton, ACT 2600, Australia
[†] Present address: Centre for Crop Systems Analysis, Wageningen University & Research, PO Box 430, 6700 AK, Wageningen, Netherlands.

* Correspondence: yazen.al-salman@wur.nl

Received 19 June 2024; Editorial decision 2 October 2024; Accepted 7 October 2024

Editor: Tracy Lawson, University of Essex, UK

Abstract

Environmental change requires more crop production per water use to meet the rising global food demands. However, improving crop intrinsic water use efficiency (iWUE) usually comes at the expense of carbon assimilation. Sorghum is a key crop in many vulnerable agricultural systems with higher tolerance to water stress (WS) than most widely planted crops. To investigate physiological controls on iWUE and its inheritance in sorghum, we screened 89 genotypes selected based on inherited haplotypes from an elite line or five exotics lines, containing a mix of geographical origins and dry versus milder climates, which included different aquaporin (AQP) alleles. We found significant variation among key highly heritable gas exchange and hydraulic traits, with some being significantly affected by variation in haplotypes among parental lines. Plants with a higher proportion of the non-stomatal component of iWUE still maintained iWUE under WS by maintaining photosynthetic capacity, independently of reduction in leaf hydraulic conductance. Haplotypes associated with two AQPs (SbPIP1.1 and SbTIP3.2) influenced iWUE and related traits. These findings expand the range of traits that bridge the trade-off between iWUE and productivity in C_4 crops, and provide possible genetic regions that can be targeted for breeding.

Keywords: C_4 crops, genotypic variation, hydraulic conductance, sorghum, stomatal conductance, water stress, water use efficiency.

Introduction

Food security amid water scarcity is one of the key global challenges of the 21st century (UNCTAD, 2011). Sorghum (*Sorghum bicolor*) is globally important for fuel, fibre, food (Borrell *et al.*, 2014b), and animal feed (George-Jaeggli *et al.*, 2017). Sorghum, a C_4 species, was first domesticated in Africa, where it remains a key staple crop in the arid and semi-arid areas of sub-Saharan Africa, a region experiencing a rapid rise in population (Dillon *et al.*, 2007; Borrell *et al.*, 2014a). Such environments are heavily dependent on rainfall, which are expected to show more erratic patterns with climate change (Rippke *et al.*, 2016). With intensifying water scarcity, more attention is being paid to crop productivity per unit of transpired water (Passioura, 2006). This characteristic is termed transpiration efficiency or water use efficiency (WUE) (Passioura, 1977). At the leaf level, the physiological control of WUE is quantified as the ratio of leaf carbon assimilation (A_n) to stomatal conductance to water vapour (g_s), and termed intrinsic water use efficiency (iWUE).

Selecting for higher iWUE in breeding programmes of C_4 crops has been challenging for a number of reasons. First, iWUE is a complex trait with multiple physiological components contributing to the variations in A_n and g_s (Condon *et al.*, 2004). Secondly, there is a potential lack of heritable WUE-related traits that can be easily screened (Hammer *et al.*, 1997). Proxies for iWUE in C_3 crops such as carbon isotope discrimination are not easily applicable in C_4 counterparts (Condon and Richards, 1992; Henderson *et al.*, 1998; Rebetzke *et al.*, 2002; von Caemmerer *et al.*, 2014; Ellsworth and Cousins, 2016; Ellsworth *et al.*, 2020). Hence, finding genetic variation in iWUE among C_4 crops has mainly depended on gas exchange parameters (Xin *et al.*, 2009). Consequently, improving iWUE in C_4 crops requires a better understanding of the mechanisms leading to genetic variation in gas exchange and iWUE (Jackson *et al.*, 2016).

Achieving higher iWUE can come at the expense of photosynthesis and biomass production (Martin *et al.*, 1999; Condon *et al.*, 2004; Passioura, 2006; Blum, 2009). This is because increases in iWUE may result from restricting water use via stomatal closure, which usually occurs during water stress (WS). However, if the leaf can still maintain a high photosynthesis rate at lower intercellular [CO_2] (C_i) due to stomatal closure, then iWUE increases can benefit biomass production when water is scarce and allow water to remain in the soil for later phenological stages (Sinclair *et al.*, 2005; Vadez, 2019; Srivastava *et al.*, 2024). Still, higher g_s and water use associated with high photosynthesis has led to higher yields in a number of crops under both WS (Blum *et al.*, 1982; Sanguineti *et al.*, 1999; Araus *et al.*, 2003; Vijayaraghavareddy *et al.*, 2020; Ouyang *et al.*, 2022; de Oliveira *et al.*, 2023) and well-watered (WW) (Reynolds *et al.*, 1994; Fischer *et al.*, 1998; Horie *et al.*, 2006) conditions. Therefore, a key challenge is to understand how to screen for greater iWUE without sacrificing greater productivity, especially under WS (Leakey *et al.*, 2019; de Oliveira *et al.*, 2022, 2023).

iWUE depends on the A_n–g_s relationship, which is almost linear at low to moderate g_s, and reaches a plateau at high g_s (Wong *et al.*, 1979; Gilbert *et al.*, 2011). Consequently, A_n and g_s contribute different proportions to iWUE depending on their operational position along the A_n–g_s curve (Ghannoum, 2016). When comparing different plants, high iWUE may be due to higher A_n, and/or lower g_s (Leakey *et al.*, 2019). The operation of the CO_2-concentrating mechanism (CCM) in C_4 leaves leads to the saturation of A_n at lower C_i than in C_3 plants, and hence low g_s, which means that operating with high g_s may lose water without improving A_n (Srivastava *et al.*, 2024). On the other hand, some crop varieties can sustain high iWUE due to higher photosynthetic capacity per given C_i, and Gilbert *et al.* (2011) proposed a method to screen for variation in iWUE associated with stomatal or non-stomatal components of A_n applied to soybean (C_3 dicot) and later applied by Li *et al.* (2017) in sugarcane (C_4 monocot). Finding such varieties is agronomically beneficial as it would alleviate the often-negative relationship between iWUE and photosynthesis or productivity.

The contribution of plant or leaf water status to WS responses can also be an important determinant of the trade-off between iWUE and photosynthesis. During WS, the hydraulic flux of water from the soil to the sites of transpiration within the leaves is often reduced, leading to a decrease in plant (K_{plant}) and leaf (K_{leaf}) hydraulic conductances. Consequently, leaves close stomata to maintain cell turgor and metabolism, and to reduce the risk of catastrophic hydraulic failure (Meinzer and Grantz, 1990; Mott and Franks, 2001; Meinzer, 2002; Brodribb *et al.*, 2003), which also reduces CO_2 supply for photosynthesis. One by-product of selecting for high iWUE under WS is obtaining varieties that favour water conservation in the soil, sometimes at the cost of photosynthesis (Choudhary *et al.*, 2013; Choudhary and Sinclair, 2014). This strategy often selects varieties with low K_{leaf} or that reduce K_{leaf} significantly during WS and especially at high vapour pressure deficit (VPD). However, lower K_{leaf} negatively impacts photosynthesis either directly, or indirectly via reducing g_s and hence C_i. Hence, screening for variation in hydraulic responses to WS can identify varieties that maintain A_n despite reduced C_i under WS, attaining higher iWUE.

A possible target that link photosynthesis, water relations, and iWUE are aquaporins (AQPs) (Vadez *et al.*, 2014; Reddy *et al.*, 2015). AQPs are channel proteins embedded in the lipid bilayer of plant cellular membranes. AQPs strongly influence the flow of water and ions within the leaf, affecting physiological parameters such as K_{leaf} and iWUE (Maurel *et al.*, 2015), including in sorghum (Choudhary *et al.*, 2013; Hasan *et al.*, 2015; Liu *et al.*, 2015; Hasan *et al.*, 2017; Zhang *et al.*, 2019). More importantly, several AQPs in plants have been shown to be key CO_2 transporters (sometimes called cooporins) especially across the plasma membrane (Groszmann *et al*., 2017). Hence, they could hypothetically increase CO_2 or H_2O supply to the sites of carboxylation without increasing g_s.

Screening for variation in physiological traits is laborious and time-consuming, and requires an extensive number of genotypes. We explored the rich genetic resources that are available for sorghum (Mace *et al*., 2019), using variations in genomic regions associated with different AQP alleles (haplotypes) from a sorghum nested association mapping (NAM) population (see the Materials and methods). We curated >80 genotypes and grew them under two watering regimes to assess the degree of variation of iWUE and other plant traits in closely similar sorghum genotypes under WS and to use that variation to test the following hypotheses: (i) partitioning the stomatal and non-stomatal components of iWUE within this diversity will reveal genotypes that achieve high iWUE under WS by maintaining photosynthesis; (ii) achieving high iWUE under WS due to maintenance of photosynthesis will be underpinned by maintenance of K_{leaf} and leaf water status; and, finally, (iii) the maintenance of hydraulics and photosynthesis under WS will be linked to certain AQPs and their related haplotypes.

Materials and methods

Genotype selection

The genotypes used in this study are a part of a NAM population (Jordan *et al*., 2011; Tao *et al*., 2020). NAM is a type of selective breeding that allows for statistical robustness while retaining diversity of parental lines. NAM maintains some allelic diversity by breeding (and backcrossing) recombinant inbred lines (RILs) from multiple parents with a single parent as a reference line (Fig. 1). Hence, the progeny share most of their genetic material, and phenotypic differences can be quickly linked to specific genetic regions. Genotypes used in our study came from a sorghum NAM population that comprises an elite parental line R937945-2-2 (recurrent parent, RP) crossed with >100 exotic lines with geographical or racial diversity (non-recurrent parent, NRP). The F_1 progeny were backcrossed with the elite parent to produce BC_1F_1 populations. BC_1F_1 genotypes compromise ~22–25% exotic (NRP) line genome, with the rest being RP background (Fig. 1). Individual BC_1F_1 populations are genotyped using high-density single nucleotide polymorphism (SNP) markers providing profiles of the exact exotic chromosomal segments, giving us information on what genes are coded for in the 22–25% NRP portion of the genome, and what genes are coded for in the remaining RP section of the genome. In addition to this resource, whole-genome sequencing is available for many of the exotic parental lines and the elite line (Mace *et al*., 2013).

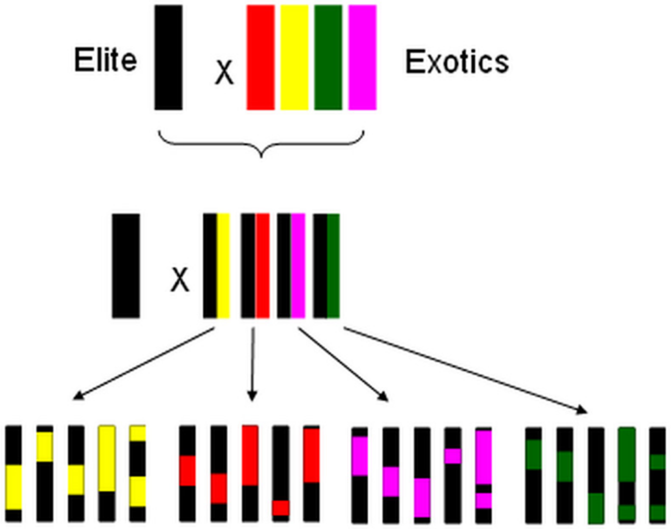

Fig. 1. A simplified illustration of how recombinant inbred lines (RILs) are produced using nested association mapping (NAM).

We screened this sorghum NAM population for genes of eight AQPs to select lines carrying non-synonymous SNP alleles of those genes. Specifically, the subpopulation was screened to identify individual lines with chromosomal segments harbouring the elite (RP) AQP allele (RP-haplotype) or the exotic (NRP) AQP allele (NRP-haplotype) of a specific AQP. The final 89 lines chosen were derived from five exotics (NRPs) containing a mix of geographical origins, with specific focus on a mix of dry versus milder climates with the idea that these would have greater extremes in the traits of interest due to necessary adaptations to their climate of origin (Table 1). This approach allowed us to create subpopulations within the 89 genotypes through focusing on one of the eight AQPs, with each subpopulation containing two sets of genotypes, a set (>5) of genotypes containing the RP-haplotype for that AQP, and a set containing the NRP-haploype. Hence, any phenotypic difference when comparing RP or NRP haplotypes associated with a certain AQP may be due to the specific AQP allele that characterizes the RP or NRP haplotype or from the accompanying genes from that chromosomal segment (haplotype), creating a link between phenotype and genotype.

Plant culture

Cylindrical pots (8 litre) were used to allow ample space for root development before implementation of the water stress treatment. The pots were adjusted to similar weight (1.5 kg) by adding gravel (100–300 mm diameter), then the same amount of soil was added to all pots. Fly screen mesh (aluminium insect screen) was added to the bottom of the pots to minimize soil seeping through pot drainage holes. The potting mix was made of soil, sand, and decomposed bark. It has large particle size for good drainage and root development. Granulated fertilizer (Osmocote Plus Organics All Purpose Fertiliser, Scotts Miracle-Gro Company, Marysville, OH, USA) was pre-mixed with the soil, with more fertilizer added in the lower half of the pot where more roots will develop as the plant grows. To each pot, 3.5 kg of soil was added, making the total pot weight 5 kg. We left 2–3 cm at the top of the pot empty, making the volume of the soil filled 7.5 litres.

Seeds were directly sown into the upper soil layer in October 2019. Plants germinated and grew in a naturally lit, controlled-environment greenhouse (Plexiglas Alltop SDP 16; Evonik Performance Materials, Darmstadt, Germany) at the Hawkesbury Institute for the Environment, Western Sydney University, Richmond, New South Wales, Australia (–33.612032, 150.749098). The ambient temperature was set at 30 °C during the day period, with night temperatures set at 18 °C. There was a 2 h period at 24 °C between the temperature transitions. The day temperature started at 08.00 h and night temperature at 20.00 h, when sunrise was about 05.00–06.00 h and sunset at 19.00–20.00 h, reaching midday maximums of 34–35 °C and midday relative humidity of 40–50% (Supplementary Fig. S1). CO_2 concentration was kept at ambient levels. Due to the large number of plants, we needed three identical and adjacent greenhouse chambers (8 m long×3 m wide×5 m tall), which contained both WW and WS pots, and pots were swapped between the three chambers every 2 weeks during growth in a randomized fashion.

Table 1. The elite (RP) and exotic (NRP) parents used in the NAM breeding programme

ID	Origin	Description
SC103-14E	South Africa	Originates from hot, dry regions of Ethiopia and Sudan.
Ai4	China breeding programme	Breeding variety not known for drought resistance.
FF_ RT×7000	US breeding programme	High yielding line that uses a lot of water and grows very well; drought sensitive.
QL12	Australia breeding programme	Australian breeding variety known for drought tolerance
IS9710	Sudan	Known for high transpiration efficiency; originated in dry regions.
R931945-2-2	Australia breeding programme	Elite parental line, the RP.

Information about the parents and the production of the NAM population can be found in Jordan *et al.* (2011).

Chamber conditions were monitored via a data logger (Tinytag plus 2, Omni Instruments) hung in the middle of the room at 2 m height. Light levels were monitored occasionally using a light meter and were 1500 μmol m^{-2} s^{-1} at midday on sunny days at plant height level at measurement time (~2 m from the ground).

Watering treatments

All plants were well watered for the first 6 weeks of growth when half of the plants by genotype were subjected to WS and the other half continued under WW conditions. When plants were 5 weeks old, pots were weighed in the late evening (W_{evening}), then watered at dusk and weighed again in the morning (W_{morning}). This allowed pots to drain excess water with minimal loss via evaporation during the night and determine pot weight at field capacity (FC) by the repetition of this routine over three consecutive sunny days and taking the average of W_{morning}. On each morning, we also measured the volumetric soil water content (VSWC) with a sensor (Campbell Scientific, Logan, UT, USA) on each pot after measuring W_{morning}. FC was 13–15% for our soil. The difference between pot weight at FC and pot weight before watering in the evening (W_{morning}–W_{evening}) represented the amount of water transpired by each plant during the day under WW conditions. After 6 weeks of growth, watering was withheld from half of the pots (WS; water stress treatment), while the other half continued to be watered at FC (WW; well-watered treatment). Stomatal conductance was monitored in WS plants until it reached ~0.1 mol m^{-2} s^{-1} or less at saturating light, with the plant also showing signs of wilting. When conductance reached the required level, and signs of wilting appeared, the VSWC was ~5% for most pots. At this point, we measured pot weight as described before to establish the amount of water lost to transpiration by the plants in the WS treatment (~50 ml). Three-fold this amount of water, equivalent to total plant transpiration during the day in the WS treatment for 3 d, was added every 3 d to the WS pots. Hence, plants under WS got just enough water for replacement of water loss via daytime evapotranspiration, and we ensured that water status of WS plants was not influenced by recent watering by the delaying of measurements to the third day after watering.

The two watering regimes were maintained until the end of the experiment, constituting the two treatments: WW—FC; WS—50 ml every day or 150 ml every 3 d. The impact of WS was visible 2 weeks after water withholding for most genotypes (plants were 8 weeks old). There were three replicates (pots) per genotype and water treatment. Hence, each genotype had six pots in total, with three for each treatment (n=3), except for the elite parent R937945-2-2 (the RP) which had six pots per treatment (n=6).

Time of measurements and sampling

Plants were sampled between weeks 9 and 12 after germination, when they had 10–12 fully expanded leaves. WS plants were measured at least 3 weeks after the onset of the drought treatment. In total, sampling lasted for about a month (mid-December 2019 to mid-January 2020), which represents the peak of the Australian summer. Priority for physiological sampling was given to plants at the booting stage so that all plants were measured before or at the start of flowering.

Midday leaf gas exchange

Midday leaf gas exchange rates were measured between 10.00 h and 14.00 h on sunny days. The photoperiod was 14–15 h and solar midday was at around 13.00–13.30 h. A Li-6400XT infrared gas analyser with an LED light source and an area of 6 cm^2 (LiCor Biosciences, Lincoln, NE, USA) was used to obtain light-saturating rates of CO_2 assimilation (A_n), stomatal conductance to water vapour (g_s), and transpiration flux (E); cuvette conditions were set at: 30 °C block temperature, flow rate of 500 μmol m^{-2} s^{-1}, photosynthetic photon flux density (PPFD) of 2000 μmol m^{-2} s^{-1} (10% blue light), ambient CO_2 concentration set to 400 ppm using a CO_2 cylinder mixer, and relative humidity of 40–60%. The leaf was inserted into the gas exchange cuvette under those conditions, avoiding the midrib and with the entire 6 cm^2 area of the cuvette filled. The leaf was left to acclimate to those conditions until gas exchange and CO_2 concentration in the substomatal cavity (intercellular CO_2, C_i) stabilized. iWUE was calculated as the ratio of A_n to g_s. All measurements were taken from the middle of the youngest fully expanded leaf (YFEL) of the plant, corresponding to the 9th–12th leaf depending on genotype. The ambient light level at the YFEL was ~500 μmol m^{-2} s^{-1}.

Leaf water potential and hydraulic conductance

A leaf adjacent to the gas exchange leaf was used to measure midday leaf water potential (Ψ_{midday}) using a Scholander-type pressure chamber (Model 1505D Pressure Chambers, PMS Instrument Company, Albany, OR, USA). The leaf below the Ψ_{midday} leaf was covered with cling wrap and aluminium foil to prevent transpiration and allow the leaf to equilibrate for at least 6 h (usually they were covered before gas exchange measurements started or the day before and collected at the end of the day and taken to the lab). This leaf was then used to estimate midday stem water potential (Ψ_{stem}). Pre-dawn leaf water potential ($\Psi_{\text{pre-dawn}}$) was sampled on different leaves before daybreak, usually taking leaves in the lower canopy. In each case, the leaf was cut at the ligule and placed in a plastic bag that was exhaled into before sealing. The bags were stored in ice boxes, then transported from the greenhouse to the lab where leaf water potentials were measured within 1–2 h of excision.

Leaf hydraulic conductance was calculated as shown in Simonin *et al.* (2015):

$$K_{\text{leaf}} = \frac{E}{(\Psi_{\text{stem}} - \Psi_{\text{midday}})} \tag{1}$$

where E refers to the leaf transpiration rate at the time of excision, estimated by measuring incident PPFD at the time of leaf excision and then E at that PPFD level estimated from light–response curves conducted on the same plant. Soil-to-leaf hydraulic conductance (referred to as plant hydraulic conductance, K_{plant}) was calculated as shown in Robson *et al.* (2012):

$$K_{\text{plant}} = \frac{E}{(\ \Psi_{\text{pre-dawn}} - \Psi_{\text{midday}})} \tag{2}$$

Leaf hydraulic resistance (R_{leaf}) was calculated as $1/K_{\mathrm{leaf}}$. Hydraulic resistance of the rest of the plant (R_{rest}) was calculated as $(1/K_{\mathrm{plant}})–R_{\mathrm{leaf}}$.

Plant and leaf morphology

Leaf width (LW) was measured at the same leaf area where gas exchange measurements were made. Leaf length (LL) was also measured. Leaf thickness (LT) was measured using a Photosynq Multispec (Photosynq, East Lansing, MI, USA). At the end of the experiment and before biomass harvest, plant height (PH) and number of leaves (LN) of each plant were recorded. In this same leaf and area of leaf for which we measured gas exchange, we collected three leaf discs of 0.5 cm^2 each to measured leaf mass per area (LMA) and relative water content (RWC). First, we placed leaf discs inside Eppendorf tubes in ice to quickly measure FW in a four positions balance, then we added distilled water and kept them in darkness and at 4 °C overnight before measuring the turgid weight (TW) again. Finally leaf discs were placed inside an oven at 65 °C for 48 h to measure DW. LMA was calculated as DW leaf discs area ($\mathrm{g\ m^{-2}}$) and RWC as: (FW–DW)/(TW–DW). Plants were harvested after 95–100 d, and total above-ground biomass was separated into panicle and vegetative (i.e. leaves and stem) to dry in an oven at 40 °C for 10 d before measuring dry biomass, but we present above-ground biomass in the data below as encompassing panicles and vegetative.

Relative chlorophyll content and quantum efficiency of PSII

Relative chlorophyll content was estimated by a SPAD meter that is embedded in the Photosynq Multispeq (Kuhlgert *et al.*, 2016). SPAD meters measure absorbance at 650 nm and 940 nm, and then relative values for chlorophyll content are produced. The Multispec was also used to record the quantum efficiency of PSII (ΦPSII) using a pulse-amplitude fluorometer at ambient light. Measurements were conducted on the same leaf as used for gas exchange.

Components of intrinsic water use efficiency

To partition the relative contribution of A_{n} and g_{s} to variation in iWUE in our population, the approach of Gilbert *et al.* (2011) was used as modified by Li *et al.* (2017). Briefly, because of the curvilinear relationship between A_{n} and g_{s}, it is expected that A_{n} and g_{s} will contribute in different proportions to iWUE depending on the position of the genotype along the curve and with respect to the mean population value.

From each measurement of gas exchange, we constructed a curve of iWUE versus g_{s} encompassing all treatments. We then calculated the average iWUE of all measurements for each treatment. To obtain variation in iWUE due to g_{s} ($\Delta\mathrm{iWUE}_{gs}$), the iWUE expected if iWUE was calculated from our reference curve (iWUE versus g_{s}, i.e. constant A_{n}) and then $\Delta\mathrm{iWUE}_{gs}$ was expressed as the deviation of the calculated iWUE from the population mean of iWUE for that treatment. This results in a value that highlights how impactful g_{s} was in deviating that genotypic iWUE from the population mean assuming fixed A_{n} (a negative value for $\Delta\mathrm{iWUE}_{gs}$ would mean that a g_{s} increase for that genotype reduced iWUE by that level compared with the mean). Variation in iWUE due to A_{n} ($\Delta\mathrm{iWUE}_{\mathrm{pc}}$; where pc stands for photosynthetic capacity)—the non-stomatal component—was then calculated as the difference between the actual measured iWUE and calculated iWUE based on g_{s} variation. Basically $\Delta\mathrm{iWUE}_{\mathrm{pc}}$ represents the remaining 'difference' between the population mean iWUE and genotypic iWUE that was not covered by $\Delta\mathrm{iWUE}_{gs}$ This means that variation in these two components can highlight how each of g_{s} and A_{n} contribute to iWUE. For example, for a given genotype, if $\Delta\mathrm{iWUE}_{gs}$ is small but $\Delta\mathrm{iWUE}_{\mathrm{pc}}$ is large (both positive), it means that iWUE is higher than the population mean because of higher photosynthesis mainly and lower conductance secondarily (see Supplementary Fig. S2 for an illustration). We also compared $\Delta\mathrm{iWUE}_{gs}$ and $\Delta\mathrm{iWUE}_{\mathrm{pc}}$ values if taken from a reference curve that is based on a reference genotypes, and it showed complete agreement (R=0.98, Supplementary Fig. S3).

Calculating the magnitude of change in A_{n} and C_{i} in response to water stress

To investigate how genotype response to WS enables the achievement of high iWUE by amplifying one of its two components highlighted earlier, we calculate the 'degree of change' in a hypothetical A_{n}–C_{i} curve based on genotype mean value change between WW and WS (Rowland *et al.*, 2023). This method estimates both the magnitude of the change and the direction of the phenotypic change vector (the angle) between two contrasting environments. The change in the angle, θ, represents change in trait covariation, in our case the dependence of A_{n} on C_{i}. Small changes in θ would indicate a large decrease in C_{i} but a small decrease in A_{n}, pointing to drought resilience, meaning the achievement of higher iWUE due to stomatal closure but also maintenance of photosynthesis rates. A large θ would indicate a combined plummeting in A_{n} with C_{i}, meaning that iWUE would increase less due to photosynthesis and more due to stomatal closure under WS (see the Results for further clarification).

Genetic variation

Broad-sense heritability was calculated as in Li *et al.* (2017):

$$H_{\mathrm{b}}^2 = \frac{\sigma_{\mathrm{g}}^2}{\sigma_{\mathrm{p}}^2} \tag{3}$$

where $\sigma_{\mathrm{g}}{}^2$ and $\sigma_{\mathrm{p}}{}^2$ are the genotypic and phenotypic variances, respectively. $\sigma_{\mathrm{g}}{}^2$ was obtained as the square of the mean from the ANOVA output. $\sigma_{\mathrm{p}}{}^2$ was calculated as:

$$\sigma_{\mathrm{p}}^2 = \sigma_{\mathrm{g}}^2 + \frac{\sigma_{\mathrm{g\times treatment}}^2}{\text{number of treatments}} + \frac{\sigma_{\mathrm{e}}^2}{\text{number of replicates}} \tag{4}$$

where $\sigma_{\mathrm{g\times treatment}}{}^2$ and $\sigma_{\mathrm{e}}{}^2$ are the genotype×treatment interaction and error variances, respectively. $\sigma_{\mathrm{g\times treatment}}{}^2$ was obtained as the mean squared of the genotype×treatment interaction and $\sigma_{\mathrm{e}}{}^2$ was obtained as the square of the mean residual error. Because the heritability analysis encompasses both treatments,he number of replicates was standardized as 5 (as opposed to 6; 3 WW and 3 WS) to account for genotypes not in both treatments. The genotypic coefficient of variation (GCV) and the phenotypic coefficient of variation (PCV) were calculated as:

$$\mathrm{GCV} = \frac{\sigma_{\mathrm{g}}}{\text{mean}} \times 100 \tag{5}$$

$$\mathrm{PCV} = \frac{\sigma_{\mathrm{p}}}{\text{mean}} \times 100 \tag{6}$$

where σ_{g} and σ_{p} are the genotypic and phenotypic standard deviation. The mean refers to the mean of all the measurements across treatments for the variable in question. For the mean value of iWUE_{gs} and $\mathrm{iWUE}_{\mathrm{pc}}$ where averages are near zero or negative (because these values are expressed as deviations from the average of all observations), the value used for mean was that for iWUE.

Statistical analyses

Statistical analysis and data visualization were performed using R software (R Core Team, 2020). Normality was checked by plotting a generalized linear model and inspecting residual plots. ANOVA and multiple ANOVA (MANOVA) were carried out using linear mixed-effects models (package nlme), with replicate and genotype as the random variable, respectively, and the fixed variables being AQP haplotype×water treatment to get the *P*-value associated with the model (Fig. 2 and Table 2, respectively). Variance within groups was performed afterwards using a post-hoc Tukey test. Regression analysis was carried in R using linear modelling (lm). A Pearson product moment correlation analysis was performed to test statistical significance of relationships at $P<0.05$ and obtain correlation coefficients *R* (which were then converted into R^2).

Results

Genotypic variation among key traits

Gas exchange variables varied among the genotypes under both watering regimes. We excluded the means for genotype R-05012-1 under WS as it responded very poorly to WS and exhibited a mean carbon assimilation rate of 1.79 µmol m^{-2} s^{-1} and stomatal conductance of 0.01 mol H_2O m^{-2} s^{-1}, which was extremely low. Mean genotype CO_2 assimilation rate (A_n) experienced a 2.2-fold variation (17.6–39.3 µmol m^{-2} s^{-1}) under WW conditions and 6.1-fold variation (6.8–32.0 µmol m^{-2} s^{-1}) under WS conditions (Table 3). Similarly, mean stomatal conductance (g_s) experienced 2.9- (0.11–0.33 mol m^{-2} s^{-1}) and 6.4-fold variation (0.01–0.16 mol m^{-2} s^{-1}) under WW and WS conditions, respectively (Table 3). Operational intercellular CO_2 concentration (C_i) was similarly variable (Table 3). iWUE experienced less variation, with a fold change of 1.9 and 1.8 under WW (92–170 µmol CO_2 mol^{-1} H_2O) and WS (121–216 µmol CO_2 mol^{-1} H_2O) conditions, respectively (Table 3).

A_n and g_s had higher GCV than iWUE and C_i (Table 3). All those variables exhibited high H_b^2 of ≥0.7 alongside hydraulic variables such as Ψ_{midday}, apart from C_i (H_b^2=0.66) (Table 3). PCV was also similarly high (30–50%) for all those variables (Table 3), indicating that environmental factors played a role in determining variation. The genotype×treatment variance was lower than the genotype variance, indicating that most genotypes responded similarly. Final harvest parameters such as above-ground biomass also varied significantly (fold change >15), and displayed high GCV and PCV (Table 3). Mean values (with the SE) of all measured variables for every genotype under both conditions are shown in Supplementary Table S1.

Influence of AQP-associated haplotypes on leaf intrinsic water use efficiency

We focused on the variation caused by differences between genotype groups with different AQP-associated haplotypes (see the Materials and methods). The results of this statistical analysis are presented in Table 2. Haplotypes associated with two AQPs, SbPIP1.1 and SbTIP3.2, had a significant impact on a number of key traits. For SbPIP1.1, the RP haplotype was associated with significantly higher A_n and g_s (Fig. 2A, B), while the NRP haplotype had higher iWUE (including its g_s component $\Delta iWUE_{gs}$) (Fig. 2C, D), LMA (Fig. 2E), and total above-ground biomass (Fig. 2F). The SbPIP1.1 NRP haplotype also had the highest $\Delta iWUE_{pc}$ of all haplotypes under WS (Supplementary Table S2; Supplementay Fig. S2H). For SbTIP3.2, The RP haplotype had higher overall A_n, g_s, SPAD, and ΦPSII (Fig. 2G, H, J, K, respectively), and higher Ψ_{midday} (Fig. 2L), especially under WS, while the NRP haplotype of SbTIP3.2 had higher iWUE and plant hydraulic resistance excluding the leaf (R_{rest}) (Fig. 2I; Table 2), without an effect on biomass. The RP haplotype of SbTIP3.2 also maintained K_{leaf} under WS (Table 2). In summary, a common trade-off was observed between photosynthesis (A_n, Φ_{PSII}) and water use (g_s, K_{leaf}) for both haplotypes. Hence, genes in that chromosomal region (haplotype) probably influence those traits, including the AQP gene.

Water stress increased iWUE, which was positively associated with above-ground biomass

Taking together all the genotypes, we observed that A_n and g_s correlated positively as expected (R^2=0.91; $P<0.0001$; Fig. 3A), with both correlating negatively with iWUE (R^2=0.92; $P<0.0001$; Fig. 3B), especially under WS for A_n (R=0.61; $P<0.0001$; Fig. 3C). A_n correlated positively with K_{leaf} under WS (R=0.53; $P<0.0001$; Fig. 3D), and g_s increased with higher Ψ_{midday} (R^2=0.49; $P<0.0001$; Fig. 3E). Subsequently, iWUE correlated negatively with K_{leaf} (R=0.54; $P<0.0001$; Fig. 3F) as well as with more negative Ψ_{midday} and increasing R_{rest} and R_{leaf} (Supplementary Table S2). Despite this, above-ground biomass was only marginally associated with A_n when considering both WW and WS plants, but positively correlated with iWUE within each watering treatment (Supplementary Table S2). Overall the above-ground biomass production across all the genotypes under WS was regulated by a reduction in leaf area under WS (Supplementary Fig. S4D), and increasing LMA (Supplementary Table S2C).

Components of iWUE under both well-watered and water stress conditions

We separated iWUE into a component attributed to the variation in A_n ($\Delta iWUE_{pc}$) and another attributed to variation in g_s ($\Delta iWUE_{gs}$) (Supplementary Fig. S2). The two components did not correlate with each other (Fig. 4A), but both positively correlated with iWUE (R=0.45–0.7, $P<0.0001$; Fig. 4C, D). $\Delta iWUE_{gs}$ was significantly higher under WW than $\Delta iWUE_{pc}$, while the opposite was true under WS (Fig. 4B). Increased iWUE associated with $\Delta iWUE_{pc}$ under WS occurs because photosynthesis decreases less than C_i (lower θ, Fig. 5A) due to the maintenance of the CCM under WS. Indeed, genotypes that increased $\Delta iWUE_{pc}$ under WS compared with WW had lower θ (R^2=0.58; $P<0.0001$; Fig. 5C), while genotypes that increased their $\Delta iWUE_{gs}$ under WS showed a weak association

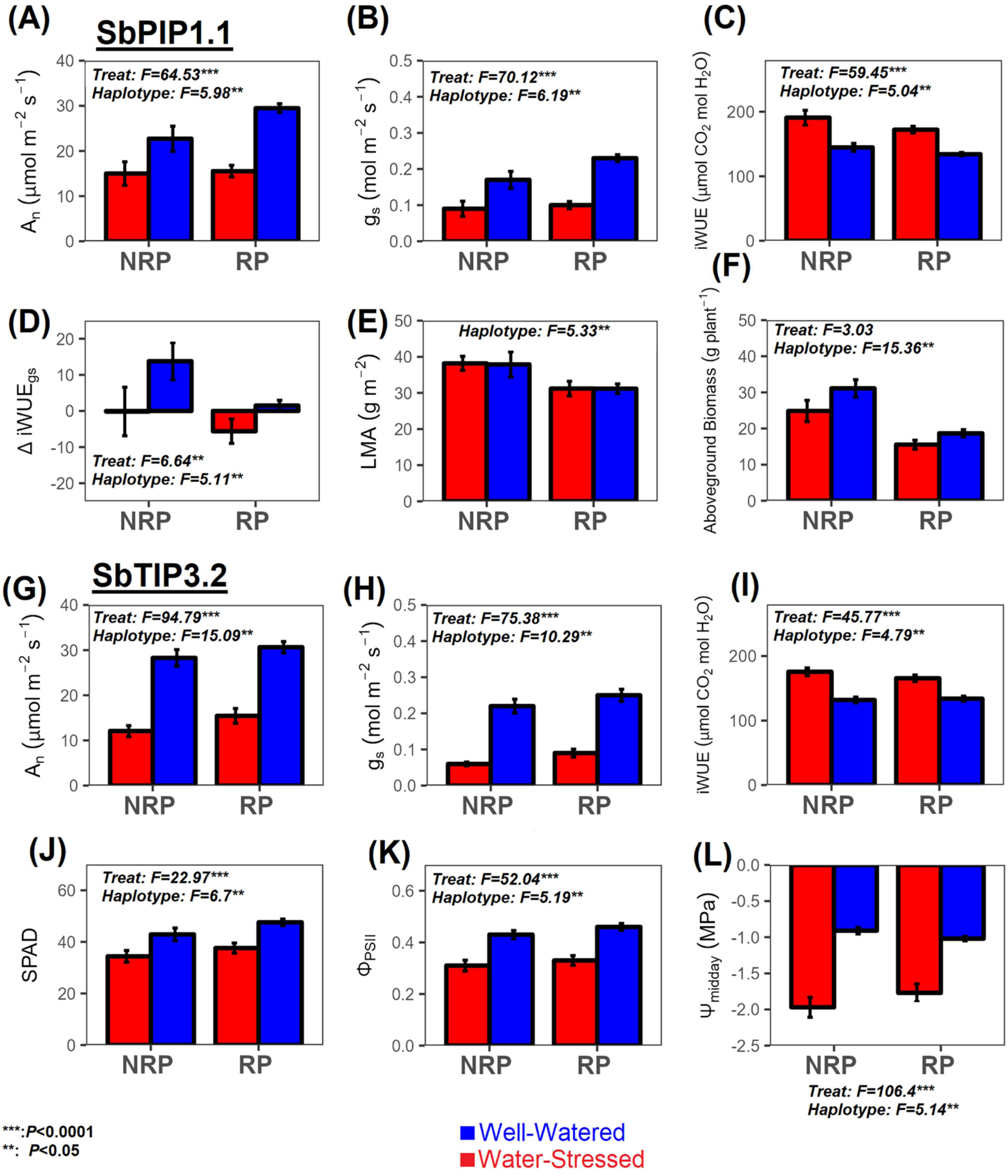

Fig. 2. Bar charts showing the effects of two aquaporin haplotypes on key traits. The two AQPs shown are those that showed significant differences in several key traits between haplotype genotype populations, with the full analysis for all AQPs shown in Table 2. Each bar represents the mean of all individual replicates belonging to the genotypes of that population (n=18–63; see Supplementay Table S3 for the number of genotypes for each haplotype×treatment combination). Statistics shown are the result of ANOVA test and post-hoc Tukey test. Bars that share the same letter have no significant differences between them at $P<0.05$. For information about the approach to genotype selection, see the Materials and methods. Each population (RP and NRP) refers to a set of genotypes that have inherited the AQP haplotype block either from the elite parent (RP) or from the exotic parent (NRP). The traits shown are (A and G) carbon assimilation rate (A_n); (B and H) stomatal conductance (g_s); (C and I) intrinsic water use efficiency (iWUE); (D) variation in iWUE due to g_s ($\Delta iWUE_{gs}$); (E) leaf mass per area (LMA); (F) above-ground biomass; (J) leaf chlorophyll content (SPAD); (K) operating efficiency of PSII (Φ_{PSII}); (L) midday leaf water potential (Ψ_{midday}).

Table 2. Summary of *P*-values from the mixed effect MANOVA of the parameters

Exotic parent	Aquaporin	Comparison	df	A_n	g_s	iWUE	ΦPSII	Ψ_{midday}	K_{leaf}	LMA	R_{leaf}	R_{rest}	SPAD	Tot Biom	$\Delta iWUE_{gs}$	$\Delta iWUE_{pc}$
FF_RT×7000	PIP 2.7	Population	1	ns	ns	ns	ns	ns	ns	ns	ns	ns	ns	ns	ns	ns
		Treatment	1	**0.0001**	**0.0001**	**0.0001**	ns	**0.0001**	**0.08**	ns	**0.0075**	**0.0015**	**0.06**	ns	**0.04**	**0.03**
		Population×Treatment	1	ns	ns	ns	ns	ns	ns	ns	ns	**0.053**	ns	ns	ns	ns
QL12	TIP 1.1	Population	1	ns	ns	ns	ns	ns	ns	ns	ns	ns	ns	ns	ns	ns
		Treatment	1	**0.0001**	**0.0001**	**0.0001**	**0.0001**	**0.0001**	**0.0017**	ns	**0.0002**	**0.0001**	**0.0001**	ns	ns	ns
		Population×Treatment	1	ns	ns	ns	ns	ns	ns	ns	ns	ns	ns	ns	ns	ns
QL12	TIP 3.2	Population	1	**0.0011**	**0.0049**	**0.04**	**0.035**	**0.036**	ns	ns	ns	**0.018**	**0.019**	ns	ns	ns
		Treatment	1	**0.0001**	**0.0001**	**0.0001**	**0.0001**	**0.0001**	**0.0001**	ns	**0.0003**	**0.0001**	**0.0001**	ns	ns	ns
		Population×Treatment	1	ns	ns	ns	ns	**0.07**	**0.03**	ns	**0.051**	ns	ns	ns	ns	ns
SC103-14E	TIP 4.3 and 4.4	Population	1	ns	ns	ns	**0.058**	ns	ns	ns	ns	ns	**0.044**	ns	ns	ns
		Treatment	1	**0.0001**	**0.0001**	**0.0001**	**0.0001**	**0.0001**	ns	ns	**0.019**	**0.012**	**0.05**	**0.0036**	ns	ns
		Population×Treatment	1	ns	ns	ns	ns	ns	ns	ns	ns	ns	ns	ns	ns	ns
IS9710	TIP 2.1	Population	1	ns	ns	ns	ns	ns	ns	ns	ns	ns	ns	ns	ns	ns
		Treatment	1	**0.0001**	**0.0001**	**0.0001**	**0.0001**	**0.0001**	**0.0001**	ns	**0.0066**	**0.011**	**0.0001**	**0.06**	**0.002**	**0.001**
		Population×Treatment	1	ns	ns	ns	ns	ns	ns	ns	ns	ns	ns	ns	ns	ns
Ai4	PIP 2.10	Population	1	ns	ns	ns	ns	ns	ns	ns	ns	ns	ns	ns	ns	ns
		Treatment	1	**0.0001**	**0.0001**	**0.0001**	**0.0001**	**0.0001**	**0.0001**	ns	**0.039**	ns	**0.0001**	**0.02**	ns	ns
		Population×Treatment	1	0.05	ns	ns	ns	ns	ns	ns	ns	ns	ns	ns	ns	ns
IS9710	PIP 1.6	Population	1	ns	ns	ns	ns	ns	ns	ns	ns	ns	ns	ns	ns	ns
		Treatment	1	**0.0001**	**0.0001**	**0.0001**	**0.0001**	**0.0001**	**0.0048**	ns	**0.0071**	**0.0081**	**0.0001**	**0.03**	**0.02**	**0.015**
		Population×Treatment	1	ns	ns	ns	ns	ns	ns	ns	ns	ns	ns	ns	ns	ns
IS9710	PIP 1.1	Population	1	**0.02**	**0.02**	**0.03**	ns	ns	ns	**0.03**	ns	ns	ns	**0.0007**	**0.035**	ns
		Treatment	1	**0.0001**	**0.0001**	**0.0001**	**0.0001**	**0.0001**	**0.0044**	ns	**0.0043**	**0.0086**	**0.0001**	**0.03**	**0.012**	**0.01**
		Population×Treatment	1	ns	ns	ns	ns	ns	ns	ns	ns	ns	ns	ns	ns	ns

Bold indicates *P*-values <0.05). Population refers to the comparison between genotypes that have the recurrent parent (RP) haplotype for the AQP and genotypes that have the non-recurrent parent (NRP) haplotype for that AQP. Treatment means the watering level: well-watered and water-limited. Both comparison have two levels (df=1). *n* (6–63), for the number of independent genotypes per haplotype group for each specific AQP see Supplementary Table S3.

Abbreviations: A_n, carbon assimilation rate; g_s, stomatal conductance; iWUE, instantaneous water use efficiency; ΦPSII, operating quantum yield of PSII; Ψ_{midday}, midday leaf water potenial; K_{leaf}, leaf hydraulic conductivity; LMA, leaf mass per area; R_{leaf}, hydraulic resistance of plant leaf; R_{rest}, hydraulic resistance of rest of the plant; SPAD, relative chlorophyll content using SPAD; Tot Biom, total above-ground biomass; $\Delta iWUE_{gs}$, iWUE attributed to variation in g_s; $\Delta iWUE_{pc}$, iWUE attributed to variation in A_n.

Table 3. Statistical summary of measured traits along with the calculated heritability and genetic variation information.

Trait	Mean	Fold change WW	Fold change WS	Genotypic variance	Treatment variance	G×T interaction variance	Residual error variance	Phenotypic variance	H_b^2	GCV (%)	PCV (%)
A_n (µmol m^{-2} s^{-1})	23.2	2.23	6.05	127.2	14 436.1	61.6	61.49	160.03	0.79	48.61	54.53
g_s (mol m^{-2} s^{-1})	0.17	2.89	6.35	0.01	1.22	0	0.01	0.01	0.75	58.82	67.92
iWUE	148.35	1.86	1.78	963	102 434	570	643.17	1281.63	0.75	20.92	24.13
C_i (µmol m^{-2} s^{-1})	111.14	2.83	6.31	2214	91 498	2170	2011.93	3339.72	0.66	42.34	52
ΦPSII	0.39	1.79	2.33	0.01	0.89	0.01	0.01	0.02	0.71	29.24	34.72
SPAD	39.48	1.92	3.21	177.8	5760.2	134.4	78.63	238.33	0.75	33.77	39.1
Ψ_{midday} (–MPa)	-1.26	2.25	2.57	0.25	46.64	0.16	0.17	0.34	0.74	39.76	46.07
$\Psi_{pre\text{-}dawn}$ (–MPa)	-0.41	14.28	14.62	0.34	40.87	0.31	0.23	0.49	0.69	141.38	169.92
Leaf width (cm)	4.54	2.35	2.3	2.16	4	1.01	1.41	2.78	0.78	32.37	36.72
LMA (g m^{-2})	32.01	2.72	2.92	123.76	64.88	86.59	121.6	176.94	0.7	34.75	41.56
RWC (%)	80.52	1.29	1.69	69.28	2458.99	111.08	102.72	126.85	0.55	10.34	13.99
Above-ground biomass (g per plant)	21.02	15.59	15.28	209.56	2749.22	155.35	138..14	314.863	0.67	68.87	84.42

A_n, carbon assimilation rate; g_s, stomatal conductance; iWUE, intrinsic water use efficiency; C_i, substomatal carbon dioxide concentration; ΦPSII, operating quantum yield of PSII; SPAD, chlorophyll content measured by SPAD; Ψ_{midday}, midday leaf water potential; $\Psi_{pre\text{-}dawn}$, pre-dawn leaf water potential; LMA, leaf mass per area; RWC, leaf relative water content; Above-ground biomass, total above-ground biomass; H_b, broad-sense heritability; GCV, genetic coefficient of variation; PCV, phenotypic coefficient of variation.

with increasing θ (R=0.4; P<0.05; Fig. 5B). Hence, genotypes that maintained photosynthetic capacity under low C_i can combine iWUE with photosynthetic performance under WS.

We examined the link between increased ΔiWUE$_{pc}$ under WS and a better hydraulic response. No correlation was found between the increase in ΔiWUE$_{pc}$ under WS and higher K_{leaf} (Fig. 6B). Instead, increasing ΔiWUE$_{gs}$ was associated with lower K_{leaf} (R=0.43; P<0.05; Fig. 6A) and more negative Ψ_{midday} (Supplementary Fig. S5C), but this did not apply to ΔiWUE$_{pc}$ (Supplementary Fig. S5D).

Discussion

This study screened a large number of sorghum genotypes that shared most of their genetic composition but differed in key gene blocks (haplotypes) that are associated with certain AQP genes inherited from the elite or exotic parental lines. This population was used to test for genetic variation in the response of iWUE and its components to WS, and their relationship with productivity and plant hydraulics. Our key findings were: (i) there was significant diversity in many variables related to productivity which also presented high broad-sense heritability; (ii) some of this diversity is underpinned by differences in haplotypes associated with some AQPs especially for gas exchange and hydraulic parameters; (iii) the non-stomatal component of iWUE (ΔiWUE$_{pc}$) was associated with higher iWUE under both WW and WS conditions; and (iv) genotypes with higher ΔiWUE$_{pc}$ were not sensitive to low K_{leaf} under WS. We discuss those findings below.

Breeding for high iWUE and possible impact of SbAQPs

Breeding for high iWUE in C_4 crops, and particularly in sorghum, has been discouraged due to lack of sufficient variation among genotypes reported in earlier studies, lack of traits that could be easily measured in large-scale screens, and the complex physiology of iWUE, where its components such as g_s can be easily influenced by environmental factors such as VPD or WS (Condon *et al.*, 2004; Sinclair *et al.*, 2005). High H_b^2 of key parameters such as A_n, g_s, iWUE, LW, and SPAD under environmental variation within inbred sorghum genotypes is a significant finding [Table 3; see similar high H_b^2 in other C_4 crops (Basnayake *et al.*, 2015; Jackson *et al.*, 2016; Li *et al.*, 2017; Ferguson *et al.*, 2023, Preprint)], considering: (i) the genotypes shared 75% of their genetic material (Fig. 1); (ii) later attempts at finding variation in iWUE were not always promising (Hammer *et al.*, 1997; Blum, 2009; Leakey *et al.*, 2019; Pan *et al.*, 2022; Zhi *et al.*, 2022; Al-Salman *et al.*, 2023); and (iii) previous key improvements in sorghum, such as the stay-green trait, were achieved via a significant breeding contribution from wild sorghum relatives (Ochieng *et al.*, 2021). Despite the high H_b^2, the high PCV of iWUE (Table 3) meant that environmental factors that affect g_s played an important role in driving variation of iWUE.

Hence, success in breeding for high iWUE is dependent on understanding the effect of different adaptive traits on iWUE and, vice versa, under different environments (Reynolds *et al.*, 1994; Araus *et al.*, 2003). To screen for and expand the suite of such adaptive traits, we partitioned iWUE into a non-stomatal component (ΔiWUE$_{pc}$) and a stomatal component (ΔiWUE$_{gs}$) (as in Gilbert *et al.*, 2011 and Li *et al.*, 2017), allowing us to reconcile high iWUE with photosynthetic performance and to link iWUE components to traits such as K_{leaf} or θ. Also, the variation in iWUE we found was associated with haplotypes where specific AQP genes were positively ascribed to parental lines from contrasting geographical regions and climates. This genetic information may be used for further specific studies addressing the role of such AQPs, or the accompanying genes, in sorghum performances under both WW and WS conditions.

Our results hint at a possible role for two AQPs (SbPIP1.1 and SbTIP3.2) that might influence iWUE and related traits (Fig. 2). AQPs change the permeability of cell membranes, facilitating water transport from the apoplastic region to the inner cells, and vice versa from the xylem to the stomata in the leaves, and hence keeping leaf cells hydrated during transpiration (Shope *et al.*, 2008; Mott and Peak, 2010; Chaumont and Tyerman, 2014; Li *et al.*, 2014). Water needs to enter guard cells for stomatal opening and increasing g_s (Franks and Farquhar, 2007; Rockwell *et al.*, 2014; Buckley *et al.*, 2017), which subsequently increases A_n and reduces iWUE (Fig. 2). The ability to maintain higher g_s can be related to improved leaf hydraulic traits (Brodribb *et al.*, 2005). For example, the RP SbTIP3.2 haplotype had higher Ψ_{midday}, higher g_s, and maintained K_{leaf} under WS compared with the NRP (Fig. 2L; Table 2; Supplementary Table S3). TIP AQPs are localized in the vacuolar membrane (tonoplast) and play a key role in maintaining cell turgor, possibly explaining the effect on leaf water status of SbTIP3.2 (Chaumont and Tyerman, 2014). Ectopic expression of a TIP gene has demonstrated that increased AQP activity generally leads to anisohydric behaviour by promoting water transport within the plant and preventing stomatal closure (Maurel *et al.*, 2015). Furthermore, TIPs and PIP2s are known to transport the most abundant reactive oxygen species (H_2O_2), which may have a role in plant cell signalling and even in detoxication of reactive oxygen species (Maurel *et al.*, 2015). However, WS also alters leaf pH and triggers abscisic acid (ABA) production and transport, which impact the activity of proton pumps associated with AQP activation and probably reducing AQP expression levels (Alexandersson *et al.*, 2005; Miyazawa *et al.*, 2008; Shatil-Cohen *et al.*, 2011; Pantin *et al.*, 2013; Shivaraj *et al.*, 2021). Therefore, it is also likely that other genes within that haplotype contribute to this response. Increased A_n in RP SbTIP3.2 may be attributed to the higher g_s, but also to more efficient reactive oxygen species-scavenging systems, which is in agreement with their higher chlorophyll content (as surrogated by SPAD) and electron transport rate, as inferred by higher ΦPSII (Fig. 2J, K). We did find significant differences in those two parameters between the RP and NRP haplotypes associated with SbTIP4.3/4.4 but with no impact on A_n (Table 2). Given that SbTIP4.3/4.4 genes are located in chromosome 3, but SbTIP 3.2 and SbPIP 1.1 are in chromosome 6 close to each other (Reddy *et al.*, 2015), and that both haplotypes from the elite parental line used in the Australian breeding programme (RP SbTIP 3.2 and RP SbPIP 1.1) had higher A_n and g_s, although lower iWUE than NRP haplotypes, they can be exploited to increase A_n under predominantly WW conditions.

However, the NRP haplotype (associated with the parental line IS9710 originated from the dry region of Sudan) of the AQP SbPIP 1.1 had significantly higher ΔiWUE$_{gs}$, iWUE, above-ground biomass, and LMA than the RP SbPIP 1.1 haplotype under WW conditions, suggesting a trade-off between higher carbon assimilation by unit of leaf area of the RP Australian line, but total plant assimilation of the NRP Sudanese line. This same haplotype (NRP SbPIP1.1) had the highest ΔiWUE$_{pc}$ of all haplotypes under WS, but also the highest above-ground biomass and highest iWUE of all haplotypes under WS, suggesting a probable function of SbPIP1.1 from the Sudanese haplotype also in the WS response. Further studies are required to ascertain the functions of SbAQPs genes, and related genes associated with the haplotypes identified in this study, and the precise role of the highlighted AQPs in abiotic stress responses.

Screening for both high A_n and iWUE under water stress may be achieved through C_i and might be associated with above-ground plant biomass

In C_4 plants, increased g_s under WW conditions may not be advantageous because C_4 photosynthesis saturates close to their operational C_i, resulting in the strong dependence of iWUE on g_s (Figs 3B, 4B) as observed in previous studies (Jackson *et al.*, 2016; Cano *et al.*, 2019; Pignon *et al.*, 2021b; Pan *et al.*, 2022; Al-Salman *et al.*, 2023). Under WS, lower g_s increases iWUE overall but also imposes a diffusional limitation on A_n by lowering C_i. Hence, variation in photosynthetic capacity can overcome this diffusional limitation and increase iWUE by maximizing A_n for a given g_s (Fig. 4B), or rather C_i as shown for genotypes with higher ΔiWUE$_{pc}$ having smaller A_n reductions compared with C_i (Fig. 5C) (Collyer and Adams, 2007; Gilbert *et al.*, 2011; Li *et al.*, 2017). C_i can then be an indicator of not just iWUE, but of ΔiWUE$_{pc}$ (see strong association of C_i with ΔiWUE$_{pc}$ compared with ΔiWUE$_{gs}$ in Supplementary Table S2), confirming previous assumptions about C_i as an integrator of iWUE and productivity in C_4 plants (Ghannoum, 2016; Jackson *et al.*, 2016; Condon, 2020). However, we found no strong relationship between A_n or ΔiWUE$_{pc}$ and biomass, apart from a weak relationship between A_n and panicle size

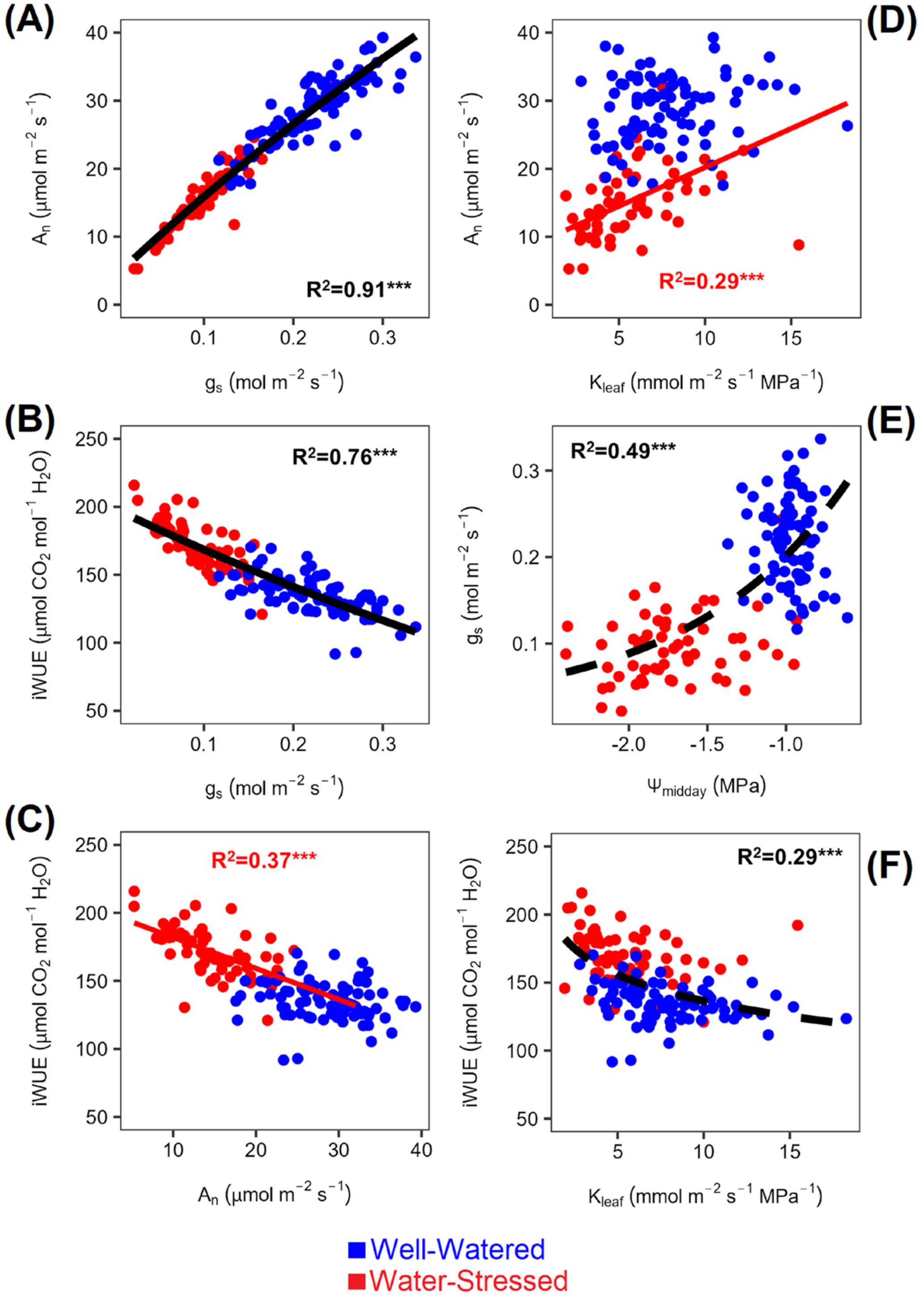

Fig. 3. Relationship between leaf gas exchange parameters and hydraulic parameters. Data were collected on the YFEL and measured at saturating light levels (see the Materials and methods). Each point in scatter plots represents the genotype mean (n=3). The SE is presented in Supplementary Table S1. R^2 values and related significant levels (***P<0.0001; **P<0.05) are from a Pearson product–moment correlation analysis or from the exponential fit models. Leaf water potential measurements were collected from the leaf adjacent to the YFEL used for gas exchange. (A) Net carbon assimilation rate (A_n) versus stomatal conductance (g_s); (B) intrinsic water use efficiency (iWUE) versus g_s; (C) iWUE versus A_n; (D) A_n versus leaf hydraulic conductance (K_{leaf}); (E) g_s versus midday leaf water potential (Ψ_{midday}); (F) iWUE versus K_{leaf}.

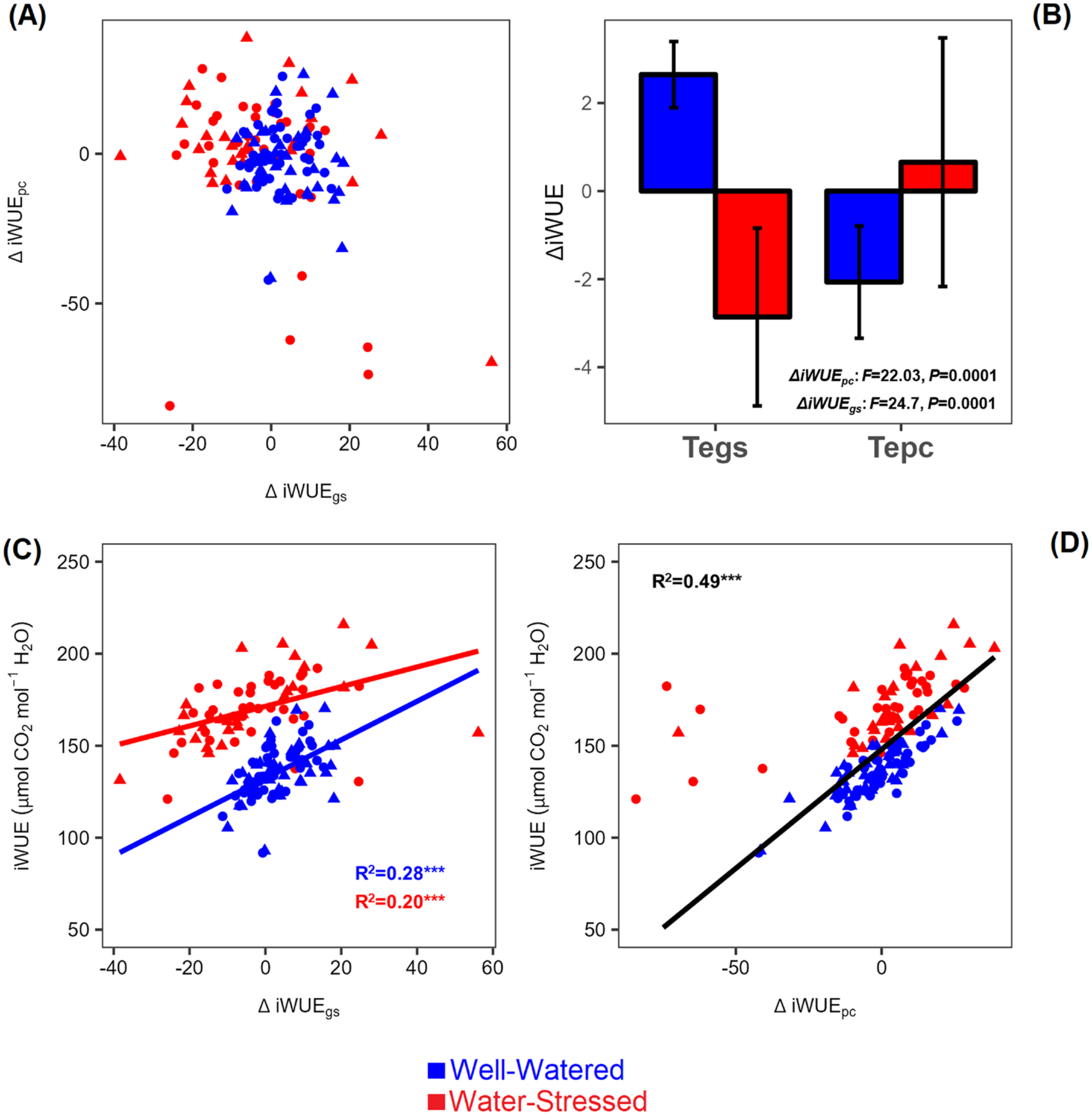

Fig. 4. The distribution of the components of intrinsic water use efficiency (iWUE) and their relationship with each other. The values in each scatter plot compromise the mean of every genotype (*n*=3) per treatment. For the bar chart, the mean is of the genotype population (*n*=89 for WW and *n*=61 for WS). Data were collected on the YFEL and measured at saturating light levels (see the Materials and methods). Each point in scatter plots represents the genotype mean (*n*=3). The SE is presented in Supplementary Table S1. R^2 values and related significant levels (***P<0.0001; **P<0.05) are from a Pearson product–moment correlation analysis or from the exponential fit models. R^2 values are from a Pearson product–moment correlation analysis. (A) Variation in iWUE due to stomatal conductance (ΔiWUE$_{gs}$) versus variation in iWUE due to photosynthetic capacity (ΔiWUE$_{pc}$); (B) bar chart showing the treatment effect on ΔiWUE$_{gs}$ and ΔiWUE$_{pc}$; (C) iWUE versus ΔiWUE$_{gs}$; (D) iWUE versus ΔiWUE$_{pc}$.

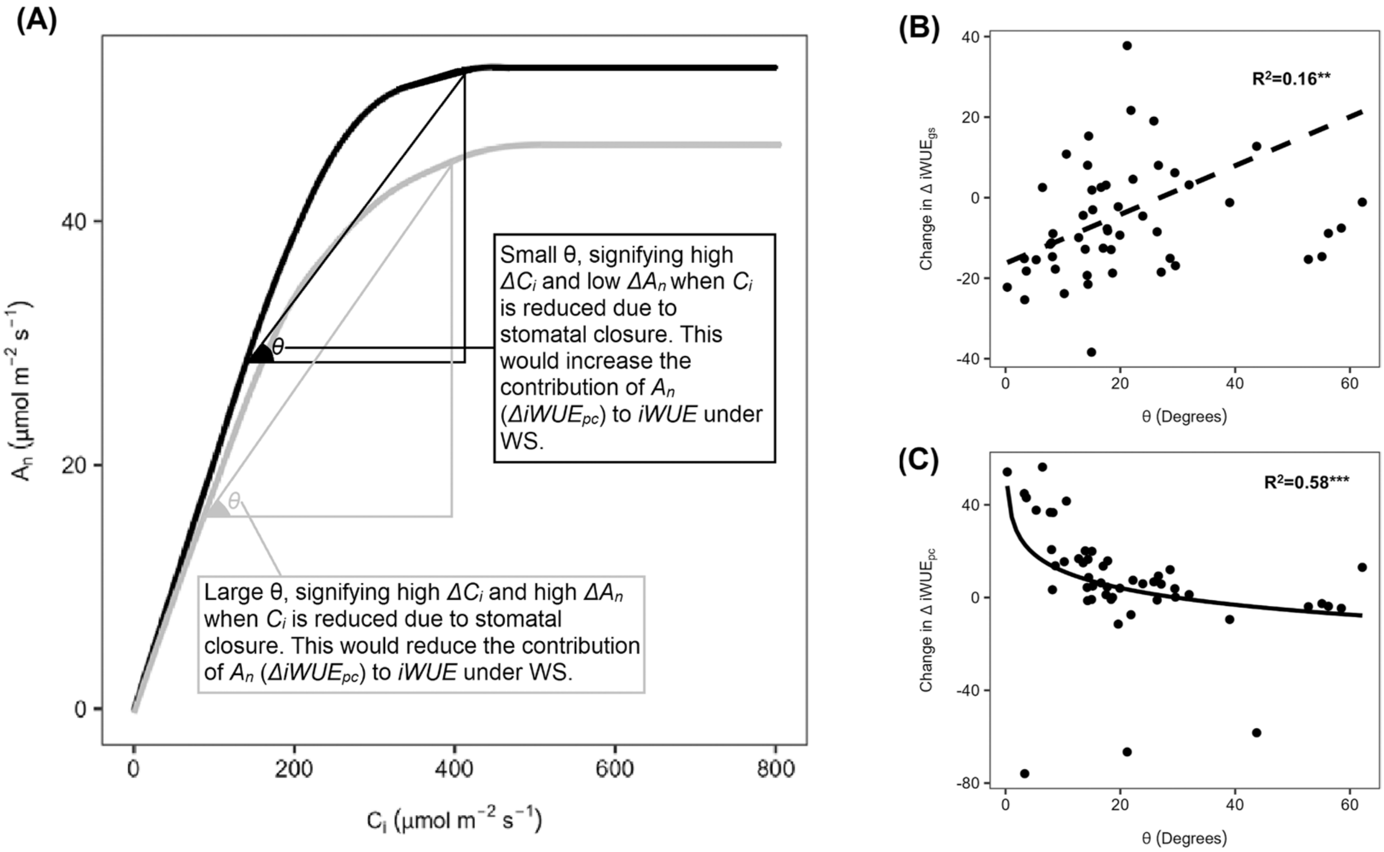

Fig. 5. Relationship between components of intrinsic water use efficiency (iWUE) and the photosynthetic response to water limitation. (A) Conceptual representation of the change in net assimilation rate (A_n) versus the operational intercellular CO$_2$ concentration (C_i) under progressive water stress driven mainly by stomatal limitation (black curve) or by a concomitant decrease in both stomatal and non-stomatal limitations (grey line). The figure shows potential change in C_i (ΔC_i), the accompanying change in A_n (ΔA_n), and the degree of change in the A_n–C_i relationship [the angle θ, with $\theta = \tan^{-1}(\Delta A_n/\Delta C_i)$] when the plant experiences water limitation. (B and C) Relationship between degree of change in the A_n–C_i relationship (θ) from WW to WS with the change in the contribution of each component of intrinsic water use efficiency [i.e. iWUE variation due to stomatal conductance (ΔiWUE$_{gs}$) and non-stomatal conductance or photosynthetic capacity (ΔiWUE$_{pc}$)] also between WW and WS (i.e. WS–WW). Data were collected on the YFEL and measured at saturating light levels (see the Materials and methods). Each point in scatter plots represents the genotype mean (n=3). The SE is presented in Supplementary Table S1. R^2 values and related significant levels (*** P<0.0001; ** P<0.05) are from a Pearson product–moment correlation analysis or from the exponential fit models.

when both treatments are grouped (Supplementary Table S2A). We also detected a weak (R=0.27) but statistically significant relationship between iWUE and total biomass (Supplementary Table S1B, C). We note here that the significant, but low R^2 (and R) values displayed in our data are typical of studies focused on intra-specific diversity especially within crops and especially when exploring complex physiological traits that are underpinned by several processes (Pignon *et al.*, 2021a; Li *et al.*, 2022; Zhi *et al.*, 2022).

Efficient use of water at the leaf scale [higher leaf Ψ_{midday} and lower plant hydraulic resistance (R_{rest}) (Supplementary Table S2B, C)] combined with morphological adaptations such as narrower leaves (Supplementary Fig. S4A) and higher leaf density [as LMA increased but leaf thickness only marginally reduced under WS (Supplementary Fig. S4C, D)] can lead to reduced g_s [see positive association between g_s and LW in Supplementary Table S2 also found in Pan *et al.* (2022) and Al-Salman *et al.* (2023)]. This results in reduced water use and high iWUE, leading to water conservation in the soil for biomass accumulation later in the season (Seneweera *et al.*, 2001; Vadez, 2019). Previous work on stay-green sorghum (most of our population is stay-green) showed that plant water use is lower during vegetative and early-reproductive stage, which is when we measured gas exchange, before ramping up during grain filling (Borrell *et al.*, 1999, 2014a, b, George-Jaeggli *et al.*, 2017). There is still scepticism about how much iWUE or photosynthesis *per se* can help drive productivity in future environments (Sinclair, 2012; Sinclair *et al.*, 2019), especially in C$_4$ crops (Sales *et al.*, 2021), since the yield of grain crops is heavily influenced by changing source–sink relationships and seasonal timings (Dingkuhn *et al.*, 2020; Fabre *et al.*, 2020). The impact of leaf-level physiological traits on whole-plant productivity under different conditions requires a comprehensive approach (Sreeman *et al.*, 2018; Tardieu *et al.*, 2018).

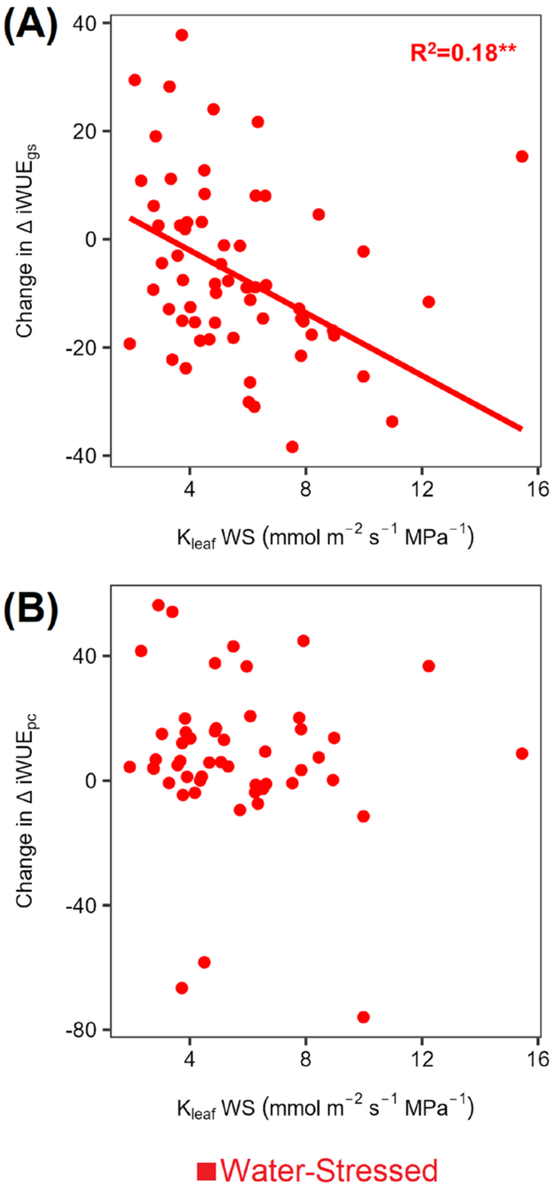

Fig. 6. Relationship between the change in the contribution of each component of intrinsic water use efficiency from WW to WS (i.e. WS–WW) with leaf hydraulic conductance (K_{leaf}) under WS. Data were collected on the YFEL and measured at saturating light levels (see the Materials and methods). Each point in scatter plots represents the genotype mean (*n*=3). The SE is presented in Supplementary Table S1. R^2 values and related significant levels (***P<0.0001; **P<0.05) are from a Pearson product–moment correlation analysis or from the exponential fit models. Leaf water potential measurements were collected from the leaf adjacent to the YFEL used for gas exchange. (A) Change in iWUE variation due to stomatal conductance (ΔiWUE$_{gs}$) versus K_{leaf} WS; (B) change in iWUE variation due to photosynthetic capacity (ΔiWUE$_{pc}$) versus K_{leaf} WS.

Road map to select promising sorghum genotypes under soil water deficit

A comprehensive physiological approach to crop drought response requires understanding of the relevant traits in response to the specific environment (Tardieu *et al.*, 2018). Too high iWUE under soil water deficit due to lowering g_s is not desirable because this indicates that the plant is experiencing moderate to severe WS and has an overall lower plant water status and reduced K_{leaf} (Blum, 2009; Sinclair, 2012, 2018). Indeed, reductions of K_{leaf} and Ψ_{midday} were associated with increasing ΔiWUE$_{gs}$ (and more closed stomata) [Fig. 6A; Supplementary Fig. S5C; Supplementary Table S2, coming at the expense of photosynthesis (see negative correlation between ΦPSII and ΔiWUE$_{gs}$ under WS (Supplementary Fig. S5A)]. Higher K_{leaf} can help maintain A_n under low C_i. Selecting for genotypes that respond to soil drought by taking some hydraulic 'risks' (maintaining K_{leaf}) and keeping stomata relatively open under increasing WS may increase iWUE by increasing carbon accumulation as seen already in some grasses (Holloway-Phillips and Brodribb, 2011). Such a genotype would operate where the minimum g_s is attained for the maximum A_n (hence, high iWUE associated with high ΔiWUE$_{pc}$) (Fig. 5). Traits that enable 'risky' hydraulic behaviour without risk of cavitation can include deeper and more conductive roots, wider xylem vessels (Scoffoni *et al.*, 2011), and higher leaf vein density [already associated with higher iWUE in sorghum (Pan *et al.*, 2022; Al-Salman *et al.*, 2023)]. Other important traits can be related to extra-xylem conductivities such as enhanced mesophyll conductance (of CO_2 or H_2O), reduced bundle sheath conductance, reduced airspace, and more compact mesophyll structure around veins (Buckley, 2015; Buckley *et al.*, 2015; Sack *et al.*, 2015; Fiorin *et al.*, 2016; Xiong *et al.*, 2017, 2018; Pathare *et al.*, 2020; Al-Salman *et al.*, 2023), which are all processes influenced by AQPs (Maurel *et al.*, 2015; Negin and Moshelion, 2016; Groszmann *et al.*, 2017; Ermakova *et al.*, 2021). Combining water use strategy with gas exchange mechanisms is crucial to clarifying the benefits of increasing iWUE under different conditions (Liang *et al.*, 2023).

Conclusion

We conducted a physiologically extensive screen of >80 sorghum genotypes selected based on differences in haplotypes originating from different parents from different origins and climates. We found significant variation among key traits, with some underpinned by differences between AQP-associated haplotypes inherited from an elite and exotic parent, providing possible target genomic regions for beneficial traits. Partitioning the components of iWUE into stomatal and non-stomatal components of A_n allowed us to find a physiological mechanism that can lead to attainment of high iWUE without hindering photosynthesis or drought tolerance. We explained this mechanism through the connection between leaf and plant hydraulic conductivities and the maintenance of assimilation rates under low C_i. These findings provide a possible roadmap to expand the range of traits linked to iWUE in C_4 crops, offer possible avenues to bridge the trade-off between iWUE and productivity, and strengthen the case for AQPs as possible key players in this endeavour.

Supplementary data

The following supplementary data are available at *JXB* online.

Table S1. Variable means with SE for each genotype at each treatment.

Table S2. Pearson correlation matrix of all the variables.

Table S3. Means for all traits for each RP/NRP AQP haplotype group.

Table S4. ANOVA comparison of parameters between chambers.

Fig. S1. Average diurnal glasshouse conditions.

Fig. S2. Calculation of different iWUE components

Fig. S3. Correlation between iWUE components calculated based on a global reference curve and a genotype reference.

Fig. S4. Boxplots of plant morphological parameter distributions across the two treatments.

Fig. S5. Relationship between components of iWUE and leaf water potential and photosynthetic efficiency.

Fig. S6. Bar charts showing the effects of water stress on iWUE components in different haplotypes.

Fig. S7. Relationship between carbon assimilation, chlorophyll content, and efficiency of PSII.

Fig. S8. Relationship between the change in the carbon assimilation–intercellular CO_2 concentration relationship and components of iWUE.

Fig. S9. Relationship between change in components of iWUE and change in hydraulic conductivity.

Fig. S10. Relationships between hydraulic conductivity and water potentials.

Fig. S11. Boxplots of gas exchange parameter distributions across the two treatments.

Fig. S12. Boxplots of hydraulic parameter distributions across the two treatments.

Acknowledgements

We would like to thank Alan Cruickshank and Dr Colleen Hunt for help with genotype selection and advice on analysis, Dr Agnieszka Wujeska-Klause, Dr Zineb Choury, and Nicole Dunn for their invaluable help during data collection, and Dr Andrew Gherlenda for technical help during project execution.

Author contributions

YA and FJC: designed the experiment based on original ideas by FJC, MG, and OG; EM: oversaw genotype selection together with DJ and MG; YA: led data collection alongside FJC; YA: analysed all the data and wrote the manuscript with help from all the authors; OG: oversaw project execution.

Conflict of interest

The authors declare no conflicts of interest.

Funding

This work was funded by the ARC Centre of Excellence for Translational Photosynthesis (grant no. CE140100015). FJC acknowledges grant RYC2021-035064-I funded by MCIN/AEI/10.13039/501100011033 and 'European Union NextGenerationEU/PRTR'.

Data availability

The data generated and analysed for this study are available from the corresponding author on request.

References

Alexandersson E, Fraysse L, Sjövall-Larsen S, Gustavsson S, Fellert M, Karlsson M, Johanson U, Kjellbom P. 2005. Whole gene family expression and drought stress regulation of aquaporins. Plant Molecular Biology **59**, 469–484.

Al-Salman Y, Cano FJ, Pan L, Koller F, Piñeiro J, Jordan D, Ghannoum O. 2023. Anatomical drivers of stomatal conductance in sorghum lines with different leaf widths grown under different temperatures. Plant, Cell & Environment **46**, 2142–2158.

Araus JL, Villegas D, Aparicio N, García del Moral LF, El Hani S, Rharrabti Y, Ferrio JP, Royo C. 2003. Environmental factors determining carbon isotope discrimination and yield in durum wheat under Mediterranean conditions. Crop Science **43**, 170–180.

Basnayake J, Jackson PA, Inman-Bamber NG, Lakshmanan P. 2015. Sugarcane for water-limited environments. Variation in stomatal conductance and its genetic correlation with crop productivity. Journal of Experimental Botany **66**, 3945–3958.

Blum A. 2009. Effective use of water (EUW) and not water-use efficiency (WUE) is the target of crop yield improvement under drought stress. Field Crops Research **112**, 119–123.

Blum A, Mayer J, Gozlan G. 1982. Infrared thermal sensing of plant canopies as a screening technique for dehydration avoidance in wheat. Field Crops Research **5**, 137–146.

Borrell AK, Bidinger FR, Sunitha K. 1999. Stay-green trait associated with yield in recombinant inbred sorghum lines varying in rate of leaf senescence. International Sorghum and Millets Newsletter **40**, 31–34.

Borrell AK, Mullet JE, George-Jaeggli B, van Oosterom EJ, Hammer GL, Klein PE, Jordan DR. 2014a. Drought adaptation of stay-green Sorghum is associated with canopy development, leaf anatomy, root growth, and water uptake. Journal of Experimental Botany **65**, 6251–6263.

Borrell AK, van Oosterom EJ, Mullet JE, George-Jaeggli B, Jordan DR, Klein PE, Hammer GL. 2014b. Stay-green alleles individually enhance grain yield in Sorghum under drought by modifying canopy development and water uptake patterns. New Phytologist **203**, 817–830.

Brodribb TJ, Holbrook NM, Edwards EJ, Gutiérrez MV. 2003. Relations between stomatal closure, leaf turgor and xylem vulnerability in eight tropical dry forest trees. Plant, Cell & Environment **26**, 443–450.

Brodribb TJ, Holbrook NM, Zwieniecki MA, Palma B. 2005. Leaf hydraulic capacity in ferns, conifers and angiosperms: impacts on photosynthetic maxima. New Phytologist **165**, 839–846.

Buckley TN. 2015. The contributions of apoplastic, symplastic and gas phase pathways for water transport outside the bundle sheath in leaves. Plant, Cell & Environment **38**, 7–22.

Buckley TN, John GP, Scoffoni C, Sack L. 2015. How does leaf anatomy influence water transport outside the xylem? Plant Physiology **168**, 1616–1635.

Buckley TN, John GP, Scoffoni C, Sack L. 2017. The sites of evaporation within leaves. Plant Physiology **173**, 1763–1782.

Cano FJ, Sharwood RE, Cousins AB, Ghannoum O. 2019. The role of leaf width and conductances to CO_2 in determining water use efficiency in C_4 grasses. New Phytologist **223**, 1280–1295.

Chaumont F, Tyerman SD. 2014. Aquaporins: highly regulated channels controlling plant water relations. Plant Physiology **164**, 1600–1618.

Choudhary S, Sinclair TR. 2014. Hydraulic conductance differences among sorghum genotypes to explain variation in restricted transpiration rates. Functional Plant Biology **41**, 270–275.

Choudhary S, Sinclair TR, Prasad PVV. 2013. Hydraulic conductance of intact plants of two contrasting sorghum lines, SC15 and SC1205. Functional Plant Biology **40**, 730–738.

Collyer ML, Adams DC. 2007. Analysis of two-state multivariate phenotypic change in ecological studies. Ecology **88**, 683–692.

Condon AG. 2020. Drying times: plant traits to improve crop water use efficiency and yield. Journal of Experimental Botany **71**, 2239–2252.

Condon AG, Richards RA. 1992. Broad sense heritability and genotype × environment interaction for carbon isotope discrimination in field-grown wheat. Australian Journal of Agricultural Research **43**, 921–934.

Condon AG, Richards RA, Rebetzke GJ, Farquhar GD. 2004. Breeding for high water-use efficiency. Journal of Experimental Botany **55**, 2447–2460.

de Oliveira JPV, Duarte VP, de Castro EM, Magalhães PC, Pereira FJ. 2022. Stomatal cavity modulates the gas exchange of *Sorghum bicolor* (L.) Moench. grown under different water levels. Protoplasma **259**, 1081–1097.

de Oliveira JPV, Duarte VP, de Castro EM, Magalhães PC, Pereira FJ. 2023. Contrasting leaf intercellular space development in sorghum and maize modulates different tolerance capacity to water limitation. Journal of Plant Research **136**, 535–548.

Dillon SL, Shapter FM, Henry RJ, Cordeiro G, Izquierdo L, Lee LS. 2007. Domestication to crop improvement: genetic resources for *Sorghum* and *Saccharum* (Andropogoneae). Annals of Botany **100**, 975–989.

Dingkuhn M, Luquet D, Fabre D, Muller B, Yin X, Paul MJ. 2020. The case for improving crop carbon sink strength or plasticity for a CO_2-rich future. Current Opinion in Plant Biology **56**, 259–272.

Ellsworth PZ, Cousins AB. 2016. Carbon isotopes and water use efficiency in C_4 plants. Current Opinion in Plant Biology **31**, 155–161.

Ellsworth PZ, Feldman MJ, Baxter I, Cousins AB. 2020. A genetic link between leaf carbon isotope composition and whole-plant water use efficiency in the C_4 grass *Setaria*. The Plant Journal **102**, 1234–1248.

Ermakova M, Osborn H, Groszmann M, *et al*. 2021. Expression of a CO_2-permeable aquaporin enhances mesophyll conductance in the C_4 species *Setaria viridis*. eLife **10**, e700095.

Fabre D, Dingkuhn M, Yin X, Clément-Vidal A, Roques S, Soutiras A, Luquet D. 2020. Genotypic variation in source and sink traits affects the response of photosynthesis and growth to elevated atmospheric CO_2. Plant, Cell & Environment **43**, 579–593.

Ferguson JN, Caproni L, Walter J, *et al*. 2023. The genetic basis of dynamic non-photochemical quenching and photosystem II efficiency in fluctuating light reveals novel molecular targets for maize (*Zea mays*) improvement. bioRxiv doi: 10.1101/2023.11.01.565118. [Preprint].

Fiorin L, Brodribb TJ, Anfodillo T. 2016. Transport efficiency through uniformity: organization of veins and stomata in angiosperm leaves. New Phytologist **209**, 216–227.

Fischer RA, Rees D, Sayre KD, Lu ZM, Condon AG, Larque Saavedra A. 1998. Wheat yield progress associated with higher stomatal conductance and photosynthetic rate, and cooler canopies. Crop Science **38**, 1467–1475.

Franks PJ, Farquhar GD. 2007. The mechanical diversity of stomata and its significance in gas-exchange control. Plant Physiology **143**, 78–87.

George-Jaeggli B, Mortlock MY, Borrell AK. 2017. Bigger is not always better: reducing leaf area helps stay-green sorghum use soil water more slowly. Environmental and Experimental Botany **138**, 119–129.

Ghannoum O. 2016. How can we breed for more water use-efficient sugarcane? Journal of Experimental Botany **67**, 557–559.

Gilbert ME, Zwieniecki MA, Holbrook NM. 2011. Independent variation in photosynthetic capacity and stomatal conductance leads to differences in intrinsic water use efficiency in 11 Soybean genotypes before and during mild drought. Journal of Experimental Botany **62**, 2875–2887.

Groszmann M, Osborn HL, Evans JR. 2017. Carbon dioxide and water transport through plant aquaporins. Plant, Cell & Environment **40**, 938–961.

Hammer GL, Farquhar GD, Broad IJ. 1997. On the extent of genetic variation for transpiration efficiency in sorghum. Australian Journal of Agricultural Research **48**, 649–655.

Hasan SA, Rabei SH, Nada RM, Abogadallah GM. 2015. Maintenance of the water use efficiency in the drought-stressed *Sorghum bicolor* L. as compared to *Zea mays* L. in relation to differential expression of aquaporin genes. Scientific Journal for Damietta Faculty of Science **4**, 55–76.

Hasan SA, Rabei SH, Nada RM, Abogadallah GM. 2017. Water use efficiency in the drought-stressed sorghum and maize in relation to expression of aquaporin genes. Biologia Plantarum **61**, 127–137.

Henderson SA, von Caemmerer S, Farquhar GD, Wade L, Hammer G. 1998. Correlation between carbon isotope discrimination and transpiration efficiency in lines of the C_4 species *Sorghum bicolor* in the glasshouse and the field. Australian Journal of Plant Physiology **25**, 111–123.

Holloway-Phillips MM, Brodribb TJ. 2011. Contrasting hydraulic regulation in closely related forage grasses: implications for plant water use. Functional Plant Biology **38**, 594–605.

Horie T, Matsuura S, Takai T, Kuwasaki K, Ohsumi A, Shiraiwa T. 2006. Genotypic difference in canopy diffusive conductance measured by a new remote-sensing method and its association with the difference in rice yield potential. Plant, Cell & Environment **29**, 653–660.

Jackson P, Basnayake J, Inman-Bamber G, Lakshmanan P, Natarajan S, Stokes C. 2016. Genetic variation in transpiration efficiency and relationships between whole plant and leaf gas exchange measurements in *Saccharum* spp. and related germplasm. Journal of Experimental Botany **67**, 861–871.

Jordan DR, Mace ES, Cruickshank AW, Hunt CH, Henzell RG. 2011. Exploring and exploiting genetic variation from unadapted sorghum germplasm in a breeding program. Crop Science **51**, 1444–1457.

Kuhlgert S, Austic G, Zegarac R, *et al*. 2016. MultispeQ Beta: a tool for large-scale plant phenotyping connected to the open photosynQ network. Royal Society Open Science **3**, 160592.

Leakey ADB, Ferguson JN, Pignon CP, Wu A, Jin Z, Hammer GL, Lobell DB. 2019. Water use efficiency as a constraint and target for improving the resilience and productivity of C3 and C4 crops. Annual Review of Plant Biology **70**, 781–808.

Li C, Jackson P, Lu X, Xu C, Cai Q, Basnayake J, Lakshmanan P, Ghannoum O, Fan Y. 2017. Genotypic variation in transpiration efficiency due to differences in photosynthetic capacity among sugarcane-related clones. Journal of Experimental Botany **68**, 2377–2385.

Li G, Santoni V, Maurel C. 2014. Plant aquaporins: roles in plant physiology. Biochimica et Biophysica Acta **1840**, 1574–1582.

Li S, Moller CA, Mitchell NG, *et al*. 2022. The leaf economics spectrum of triploid and tetraploid C_4 grass *Miscanthus* × *giganteus*. Plant, Cell & Environment **45**, 3462–3475.

Liang J, Krauss KW, Finnigan J, Stuart-Williams H, Farquhar GD, Ball MC. 2023. Linking water use efficiency with water use strategy from leaves to communities. New Phytologist **240**, 1735–1742.

Liu P, Yin L, Wang S, Zhang M, Deng X, Zhang S, Tanaka K. 2015. Enhanced root hydraulic conductance by aquaporin regulation accounts for silicon alleviated salt-induced osmotic stress in *Sorghum bicolor* L. Environmental and Experimental Botany **111**, 42–51.

Mace E, Innes D, Hunt C, Wang X, Tao Y, Baxter J, Hassall M, Hathorn A, Jordan D. 2019. The Sorghum QTL Atlas: a powerful tool for trait dissection, comparative genomics and crop improvement. Theoretical and Applied Genetics **132**, 751–766.

Mace ES, Tai S, Gilding EK, *et al*. 2013. Whole-genome sequencing reveals untapped genetic potential in Africa's indigenous cereal crop Sorghum. Nature Communications **4**, 2320.

Martin B, Tauer CG, Lin RK. 1999. Carbon isotope discrimination as a tool to improve water-use efficiency in tomato. Crop Science **39**, 1775–1783.

Maurel C, Boursiac Y, Luu D-T, Santoni V, Shahzad Z, Verdoucq L. 2015. Aquaporins in plants. Physiological Reviews **95**, 1321–1358.

Meinzer FC. 2002. Co-ordination of vapour and liquid phase water transport properties in plants. Plant, Cell & Environment **25**, 265–274.

Meinzer FC, Grantz DA. 1990. Stomatal and hydraulic conductance in growing sugarcane: stomatal adjustment to water transport capacity. Plant, Cell & Environment **13**, 383–388.

Miyazawa S-I, Yoshimura S, Shinzaki Y, Maeshima M, Miyake C. 2008. Deactivation of aquaporins decreases internal conductance to CO_2 diffusion in tobacco leaves grown under long-term drought. Functional Plant Biology **35**, 553–564.

Mott KA, Franks PJ. 2001. The role of epidermal turgor in stomatal interactions following a local perturbation in humidity. Plant, Cell & Environment **24**, 657–662.

Mott KA, Peak D. 2010. Stomatal responses to humidity and temperature in darkness. Plant, Cell & Environment **33**, 1084–1090.

Negin B, Moshelion M. 2016. The evolution of the role of ABA in the regulation of water-use efficiency: from biochemical mechanisms to stomatal conductance. Plant Science **251**, 82–89.

Ochieng G, Ngugi K, Wamalwa LN, Manyasa E, Muchira N, Nyamongo D, Odeny DA. 2021. Novel sources of drought tolerance from landraces and wild Sorghum relatives. Crop Science **61**, 104–118.

Ouyang W, Yin X, Yang J, Struik PC. 2022. Do shoot anatomical characteristics allow rice to grow well under water deficit? Journal of Agronomy and Crop Science **208**, 763–776.

Pan L, George-Jaeggli B, Borrell AK, Jordan D, Koller F, Al-Salman Y, Ghannoum O, Cano FJ. 2022. Coordination of stomata and vein patterns with leaf width underpins water use efficiency in a C_4 crop. Plant, Cell & Environment **45**, 1630.

Pantin F, Monnet F, Jannaud D, Costa JM, Renaud J, Muller B, Simonneau T, Genty B. 2013. The dual effect of abscisic acid on stomata. New Phytologist **197**, 65–72.

Passioura J. 2006. Increasing crop productivity when water is scarce—from breeding to field management. Agricultural Water Management **80**, 176–196.

Passioura JB. 1977. Grain yield, harvest index, and water use of wheat. Journal of the Australian Institute of Agricultural Science **43**, 177–120.

Pathare VS, Sonawane BV, Koteyeva N, Cousins AB. 2020. C_4 grasses adapted to low precipitation habitats show traits related to greater mesophyll conductance and lower leaf hydraulic conductance. Plant, Cell & Environment **43**, 1897–1910.

Pignon CP, Fernandes SB, Valluru R, Bandillo N, Lozano R, Buckler E, Gore MA, Long SP, Brown PJ, Leakey ADB. 2021a. Phenotyping stomatal closure by thermal imaging for GWAS and TWAS of water use efficiency-related genes. Plant Physiology **187**, 2544–2562.

Pignon CP, Leakey ADB, Long SP, Kromdijk J. 2021b. Drivers of natural variation in water-use efficiency under fluctuating light are promising targets for improvement in Sorghum. Frontiers in Plant Science **12**, 627432.

R Core Team. 2020. R: a language and environment for statistical computing. Vienna, Austria: R Foundation for Statistical Computing.

Rebetzke GJ, Condon AG, Richards RA, Farquhar GD. 2002. Selection for reduced carbon isotope discrimination increases aerial biomass and grain yield of rainfed bread wheat. Crop Science **42**, 739–745.

Reddy PS, Rao TSRB, Sharma KK, Vadez V. 2015. Genome-wide identification and characterization of the aquaporin gene family in *Sorghum bicolor* (L.). Plant Gene **1**, 18–28.

Reynolds MP, Balotac M, Delgadod MIB, Amanie I, Fischer RA. 1994. Physiological and morphological traits associated with spring wheat yield under hot, irrigated conditions. Australian Journal of Plant Physiology **21**, 717–747.

Rippke U, Ramirez-Villegas J, Jarvis A, Vermeulen SJ, Parker L, Mer F, Diekkrüger B, Challinor AJ, Howden M. 2016. Timescales of transformational climate change adaptation in sub-Saharan African agriculture. Nature Climate Change **6**, 605–609.

Robson TM, Sánchez-Gómez D, Cano FJ, Aranda I. 2012. Variation in functional leaf traits among beech provenances during a Spanish summer reflects the differences in their origin. Tree Genetics and Genomes **8**, 1111–1121.

Rockwell FE, Holbrook NM, Stroock AD. 2014. The competition between liquid and vapor transport in transpiring leaves. Plant Physiology **164**, 1741–1758.

Rowland L, Ramírez-Valiente JA, Hartley IP, Mencuccini M. 2023. How woody plants adjust above- and below-ground traits in response to sustained drought. New Phytologist **239**, 1173–1189.

Sack L, Scoffoni C, Johnson DM, Buckley TN, Brodribb TJ. 2015. The anatomical determinants of leaf hydraulic function. In: Hacke U, ed. Functional and ecological xylem anatomy. Cham: Springer, 255–271.

Sales CRG, Wang Y, Evers JB, Kromdijk J. 2021. Improving C_4 photosynthesis to increase productivity under optimal and suboptimal conditions. Journal of Experimental Botany **72**, 5942–5960.

Sanguineti MC, Tuberosa R, Landi P, Salvi S, Maccaferri M, Casarini E, Conti S. 1999. QTL analysis of drought-related traits and grain yield in relation to genetic variation for leaf abscisic acid concentration in field-grown maize. Journal of Experimental Botany **50**, 1289–1297.

Scoffoni C, Rawls M, McKown AD, Cochard H, Sack L. 2011. Decline of leaf hydraulic conductance with dehydration: relationship to leaf size and venation architecture. Plant Physiology **156**, 832–843.

Seneweera S, Ghannoum O, Conroy JP. 2001. Root and shoot factors contribute to the effect of drought on photosynthesis and growth of the C_4 grass *Panicum coloratum* at elevated CO_2 partial pressures. Australian Journal of Plant Physiology **28**, 451–460.

Shatil-Cohen A, Attia Z, Moshelion M. 2011. Bundle-sheath cell regulation of xylem–mesophyll water transport via aquaporins under drought stress: a target of xylem-borne ABA? The Plant Journal **67**, 72–80.

Shivaraj SM, Sharma Y, Chaudhary J, *et al*. 2021. Dynamic role of aquaporin transport system under drought stress in plants. Environmental and Experimental Botany **184**, 104367.

Shope JC, Peak D, Mott KA. 2008. Stomatal responses to humidity in isolated epidermes. Plant, Cell & Environment **31**, 1290–1298.

Simonin KA, Burns E, Choat B, Barbour MM, Dawson TE, Franks PJ. 2015. Increasing leaf hydraulic conductance with transpiration rate minimizes the water potential drawdown from stem to leaf. Journal of Experimental Botany **66**, 1303–1315.

Sinclair TR. 2012. Is transpiration efficiency a viable plant trait in breeding for crop improvement? Functional Plant Biology **39**, 359–365.

Sinclair TR. 2018. Effective water use required for improving crop growth rather than transpiration efficiency. Frontiers in Plant Science **9**, 1–8.

Sinclair TR, Hammer GL, Van Oosterom EJ. 2005. Potential yield and water-use efficiency benefits in sorghum from limited maximum transpiration rate. Functional Plant Biology **32**, 945–952.

Sinclair TR, Rufty TW, Lewis RS. 2019. Increasing photosynthesis: unlikely solution for world food problem. Trends in Plant Science **24**, 1032–1039.

Sreeman SM, Vijayaraghavareddy P, Sreevathsa R, Rajendrareddy S, Arakesh S, Bharti P, Dharmappa P, Soolanayakanahally R. 2018. Introgression of physiological traits for a comprehensive improvement of drought adaptation in crop plants. Frontiers in Chemistry **6**, 92.

Srivastava A, Srinivasan V, Long SP. 2024. Stomatal conductance reduction tradeoffs in maize leaves: a theoretical study. Plant, Cell & Environment **47**, 1716–1731.

Tao Y, Zhao X, Wang X, Hathorn A, Hunt C, Cruickshank AW, van Oosterom EJ, Godwin ID, Mace ES, Jordan DR. 2020. Large-scale GWAS in sorghum reveals common genetic control of grain size among cereals. Plant Biotechnology Journal **18**, 1093–1105.

Tardieu F, Simonneau T, Muller B. 2018. The physiological basis of drought tolerance in crop plants: a scenario-dependent probablistic approach. Annual Review of Plant Biology **69**, 733–759.

UNCTAD. 2011. Water for food: innovative water management technologies for food security and poverty alleviation. Geneva: United Nations.

Vadez V. 2019. Water-use efficiency. In: Ciampitti I, Prasad PVV, eds. Sorghum: state of the art and future prespectives. Madison, WI: ASA and CSSA, 267–276.

Vadez V, Kholova J, Medina S, Kakkera A, Anderberg H. 2014. Transpiration efficiency: new insights into an old story. Journal of Experimental Botany **65**, 6141–6153.

Vijayaraghavareddy P, Xinyou Y, Struik PC, Makarla U, Sreeman S. 2020. Responses of lowland, upland and aerobic rice genotypes to water limitation during different phases. Rice Science **27**, 345–354.

von Caemmerer S, Ghannoum O, Pengelly JJL, Cousins AB. 2014. Carbon isotope discrimination as a tool to explore C_4 photosynthesis. Journal of Experimental Botany **65**, 3459–3470.

Wong SC, Cowan IR, Farquhar GD. 1979. Stomatal conductance correlates with photosynthetic capacity. Nature **282**, 424–426.

Xin Z, Aiken R, Burke J. 2009. Genetic diversity of transpiration efficiency in Sorghum. Field Crops Research **111**, 74–80.

Xiong D, Douthe C, Flexas J. 2018. Differential coordination of stomatal conductance, mesophyll conductance, and leaf hydraulic conductance in response to changing light across species. Plant, Cell & Environment **41**, 436–450.

Xiong D, Flexas J, Yu T, Peng S, Huang J. 2017. Leaf anatomy mediates coordination of leaf hydraulic conductance and mesophyll conductance to CO_2 in *Oryza*. New Phytologist **213**, 572–583.

Zhang D, Zeng T, Liu X, Gao C, Li Y, Li C, Song Y, Shi Y, Wang T, Li Y. 2019. Transcriptomic profiling of sorghum leaves and roots responsive to drought stress at the seedling stage. Journal of Integrative Agriculture **18**, 1980–1995.

Zhi X, Hammer G, Borrell A, *et al*. 2022. Genetic basis of sorghum leaf width and its potential as a surrogate for transpiration efficiency. Theoretical and Applied Genetics **135**, 3057–3071.